Road traffic noise shielding by vegetation belts of limited depth

T. Van Renterghem [a,*], D. Botteldooren [1,a], K. Verheyen [2,b]

[a] Ghent University, Department of Information Technology, Sint-Pietersnieuwstraat 41, B-9000 Gent, Belgium
[b] Ghent University, Department of Forest and Water Management, Geraardsbergsesteenweg 267, B-9090 Melle-Gontrode, Belgium

ARTICLE INFO

ABSTRACT

Road traffic noise propagation through a vegetation belt of limited depth (15 m) containing periodically arranged trees along a road is numerically assessed by means of 3D finite-difference time-domain (FDTD) calculations. The computational cost is reduced by only modeling a representative strip of the planting scheme and assuming periodic extension by applying mirror planes. With increasing tree stem diameter and decreasing spacing, traffic noise insertion loss is predicted to be more pronounced for each planting scheme considered (simple cubic, rectangular, triangular and face-centered cubic). For rectangular schemes, the spacing parallel to the road axis is predicted to be the determining parameter for the acoustic performance. Significant noise reduction is predicted to occur for a tree spacing of less than 3 m and a tree stem diameter of more than 0.11 m. This positive effect comes on top of the increase in ground effect (near 3 dBA for a light vehicle at 70 km/h) when compared to sound propagation over grassland. The noise reducing effect of the forest floor and the optimized tree belt arrangement are found to be of similar importance in the calculations performed. The effect of shrubs with typical above-ground biomass is estimated to be at maximum 2 dBA in the uniform scattering approach applied for a light vehicle at 70 km/h. Downward scattering from tree crowns is predicted to be smaller than 1 dBA for a light vehicle at 70 km/h, for various distributions of scattering elements representing the tree crown. The effect of the presence of tree stems, shrubs and tree crowns is predicted to be approximately additive. Inducing some (pseudo) randomness in stem center location, tree diameter, and omitting a limited number of rows with trees seem to hardly affect the insertion loss. These predictions suggest that practically achievable vegetation belts can compete to the noise reducing performance of a classical thin noise barrier (on grassland) with a height of 1–1.5 m (in a non-refracting atmosphere).

© 2012 Elsevier Ltd. All rights reserved.

1. Introduction

The acoustical effect of a belt of trees/vegetation near roads has been a popular research topic over the past 40 years [1–10]. The conclusions drawn from such experiments are, however, often quite different. Aylor looked at sound propagation through corn, a hemlock plantation, a pine stand, and hardwood brush [1], and over dense reeds above a

---

* Corresponding author. Tel.: +32 9 264 36 34; fax: +32 9 264 99 69.
E-mail addresses: Timothy.Van.Renterghem@intec.Ugent.be (T. Van Renterghem), Dick.botteldooren@intec.Ugent.be (D. Botteldooren), Kris.Verheyen@UGent.be (K. Verheyen).
[1] Tel.: +32 9 264 99 68; fax: +32 9 264 99 69.
[2] Tel.: +32 9 264 90 27; fax: +32 9 264 90 92.

water surface [2]. He concluded that the leaf area density should be high, and leaves should be broad and thick to see significant effects. Visibility was considered to be a bad predictor of the attenuation capacity of a vegetative stand [1]. Thirty-five tree belts were studied by Fang and Ling [7]. Multiple linear regression analysis on their data showed that visibility through the vegetation and the width of the belt were the major parameters. Other parameters contributing to an improved prediction were height and length of the belt. The typical leaf size at the tested locations was considered to be rather unimportant in their regression model. Tyagi et al. [9], on the other hand, linked the significantly higher attenuation at the 3.15-kHz 1/3-octave band to the dimensions of the plant structures in their measurements. Pathak et al. [10] measured that belt width and tree height are positively correlated with traffic noise reduction. Pal et al. [6] measured near 12 vegetation belts and found that the average density and height of the plants has only a very small effect. Larger plant heights could even be negative, probably due to increased downward scattering towards receivers. Vertical and horizontal light penetration were found to be major parameters. Kragh [4] stated that the traffic noise reduction obtained by a belt of vegetation is rather limited. In his study, sound propagation through belts of vegetation was compared to sound propagation over grassland over the same distance. Significant attenuation was provided by the vegetation only above 2 kHz.

In many of the above mentioned publications, the reference situation when assessing the effect of the vegetation belts is rather unclear. Furthermore, many effects related to the interaction between sound and vegetation were jointly observed. This makes it difficult to derive design rules for vegetation belts. In this paper, numerical calculations are used to assess the effect of vegetation belts of limited width along roads. In contrast to in-situ measurements, the reference situation can be well defined and the various effects can easily be separated out. On the other hand, modeling approaches always induce some idealizations.

Basically, vegetation is able to reduce sound levels in three ways. First, sound can be reflected and scattered (diffracted) by plant elements like trunks, branches, twigs and leaves. Very close to vegetation and below tree crowns, this could lead to increased sound levels by downward scattering [11]. In many applications, however, sound energy will leave the line-of-sight between source and receiver when interacting with vegetation, leading to reduced sound pressure levels. A second mechanism is absorption caused by vegetation. This effect can be attributed to mechanical vibrations of plant elements caused by sound waves [12–14] which lead to dissipation by converting sound energy to heat. There is also a contribution to attenuation by thermo-viscous boundary layer effects at vegetation surfaces. As a third mechanism, one might also mention that sound levels can be reduced by destructive interference of sound waves. The presence of the soil can lead to destructive interference between the direct contribution from source to receiver, and a ground-reflected contribution. This effect is often referred to as the acoustical ground effect or ground dip. The presence of vegetation leads to an acoustically very soft (porous) soil, mainly by the presence of a litter layer and by plant rooting. This results in a more pronounced ground effect and in a shift towards lower frequencies compared to sound propagation over grassland [15]. As a result, this ground dip is more efficient in limiting typical engine noise frequencies (near 100 Hz) of road traffic.

Besides these direct acoustical effects, some indirect effects can be mentioned as well. Forests change the refractive state of the lower part of the atmosphere and therefore influence sound propagation as studied, e.g. in [15–18]. Near a noise barrier, a row of trees was shown to limit the screen-induced refraction of sound by the action of the wind [19,20], and the specific distribution of biomass in the canopy plays a role [21]. Fricke [22] measured that sound attenuation is influenced to an important degree by the relative humidity inside a forest, in a way that cannot be explained by the action of atmospheric absorption or by changes in soil humidity. Another type of indirect effects deals with psycho-acoustical effects. Wind-induced vegetation noise can lead to masking of unwanted sounds, and as a result, there has been interest in predicting this effect [23,24]. Traffic noise perception is also influenced by visual stimuli: with an increasing degree of urbanization (and as a result less vegetation), the perception becomes less pleasant [25].

In periodic structures, so-called acoustic band gap effects might appear (see e.g. Refs. [26,27]): Waves scattered by the components of a lattice (or the elements with a sufficient contrast in density relative to the propagation medium) interfere. This could lead to large noise reductions in particular frequency bands. The spacing between the scattering elements (lattice constant) determines the stop-band central frequencies, the filling fraction their efficiency. Applications and research mainly focus on closely packed cylinders [26–28]. An interesting question is whether such effects can be achieved by introducing periodicity in vegetation belts, keeping in mind realistic plant densities. The latter imply that the maximum filling fractions are limited. However, experiments with trees organized in periodic arrays were also found to produce attenuation peaks at frequencies below 500 Hz due to band gap effects, and not as a consequence of interaction with the ground surface as was discussed in Ref. [29]. Total traffic noise shielding was not assessed in this earlier work.

Numerical calculations with relation to sound propagation through belts of vegetation or forests all start from random orderings. In Ref. [30], tree stems were explicitly modeled in 3D with a FDTD model. In Refs. [16,18,31], multiple scattering theory for randomly spaced arrays of cylinders was used to predict sound propagation through forests.

Given the findings in recent sonic crystal research and taking into account the work reported in Ref. [29], studying periodic plant organizations seems worth the effort. Periodic planting schemes are also beneficial as regards the computational cost. 3D numerical simulations typically need a very large amount of computational resources. However, as a result of exploiting periodicity, the computational domain can be largely reduced. This is done by using mirror planes in the simulation domain, and only modeling a representative strip of the grid. Making advantage of symmetry is a sound approach in acoustical simulations, and applications of this concept are numerous. Applications of the mirror plane approach to 3D time-domain outdoor sound propagation calculations can be found, e.g. in Refs. [32,33].

A drawback of the mirror plane approach in the current context is that only planting schemes that are periodic in a direction parallel to the road axis can be modeled. From sonic crystal research, it was shown, e.g. that some defects in the lattice could be beneficial to broaden the frequency range where sound reduction is observed [34]. Orthogonal to the road axis, such effects could be included and will be studied.

As illustrated by the references in the previous paragraphs, the typical ground under vegetation could be a major effect in reducing noise. So the positive effect of the ground should preferably be preserved, and its interaction with the multiple scattering between vegetation elements should be studied. The interaction between the soil effect and the presence of scattering vegetation is not always clear when looking at literature. In Ref. [1], it was written that adding the separate effects of leaves, stems and ground to obtain the total effect for any combination of these is not unreasonable. The measurements performed in Ref. [31] lead to similar conclusions. In Ref. [15], on the other hand, it was stated that this interaction is more complicated than simply additive. Bullen and Fricke [35] found that that the largest effects of placing cylinders in their scale model of a strip of vegetation were observed above a rigid plane and for a sound frequency of 4 kHz. For an acoustically absorbing ground, the insertion loss (IL) relative to the same type of ground cover in absence of cylinders was much more moderate. Krynkin and Umnova [36] found that in their calculations of a sonic crystal made of rigid cylinders (with their axes parallel to the ground surface), the largest IL values were found for sound propagation over a rigid ground. The 3D calculations performed in this study will contribute to this discussion.

In this paper, planting schemes on a typical soil as found under vegetation, in a 15-m wide belt bordering a road, are numerically assessed. Focus is on total road traffic noise levels of light vehicles. The maximum frequency considered in this study (the 1.6-kHz one-third octave band) takes into account a relevant part of the tire/road interaction noise, and allows a more complete estimation of possible traffic noise reduction than in the related study of Heimann [30] where the maximum sound frequency that could be attained was 600 Hz.

Note that some of the modeled configurations have a tree density that would be very hard to realize in practice. However, such simulations could be helpful to reveal trends. Practical aspects will be discussed and it is indicated what configurations could be realized. Also, results will be compared to sound propagation over a grass-covered land with identical source–receiver configuration. This allows policy makers and urban planners to get a global and quantitative idea of the gain obtained by changing a piece of grassland into a tree/vegetation belt. Given the rather short propagation distance between source and receiver, refraction effects will be very limited and will not be considered here.

In addition, a simple scattering model is proposed to assess the effect of small ground-covering vegetation, shrubs, and tree crowns. One has to keep in mind that scattering by vegetation is mainly a high-frequency phenomenon since most structures in, e.g. a tree crown are very small compared to the dominant wavelengths in a road traffic noise spectrum. Furthermore, the density of the scatterers (volume fraction) is limited. Martens [37], e.g. stated that scattering by vegetation is rather unimportant when looking at total traffic noise level reduction. Measurements behind a noise barrier with and without the presence of a row of trees in Ref. [19] showed that scattering by the trees can be significant at very high frequencies (+5 dB at 10 kHz). At the 1.6 kHz one-third octave band, which will be the maximum frequency considered in this study, the amount of scattering was only near +1 dB. As a result, most important effects are expected from the presence of stems of trees (in combination with soil as appears under vegetation) which is the main concern in this paper. However, including these additional effects allows for a more complete assessment of the noise reducing effects of vegetation belts.

This paper is organized as follows. The FDTD model is briefly described in Section 2. In the next section, the choice of the simulation parameters is discussed. In Section 4, the scattering approach is presented, for the case of sound propagation through shrub layers and for tree crown scattering. In Section 5, 3D –FDTD calculation results are presented for road traffic noise shielding by vegetation belts of limited depth. In Section 6, some practical considerations concerning the feasibility of the modeled tree stands are made. In Section 7, conclusions are drawn. In the appendices, approaches aiming at reducing the computational cost are checked, and a summary of all simulations performed in this study is presented.

2. The finite-difference time-domain model

The following equations describe sound propagation in air:

$$\nabla \cdot p + \rho_0 \frac{\partial \boldsymbol{v}}{\partial t} = \boldsymbol{0}, \tag{1}$$

$$\frac{\partial p}{\partial t} + \rho_0 c_0{}^2 \nabla \cdot \boldsymbol{v} = 0. \tag{2}$$

In the linear Eqs. (1) and (2), p is the acoustic pressure, v is the particle velocity, ρ_0 is the mass density of air, c_0 is the adiabatic sound speed, and t denotes time. A homogeneous and still propagation medium is assumed. Viscosity, thermal conductivity, molecular relaxation, and gravity are neglected.

The interaction between sound waves and the soil in this study is simulated by means of the Zwikker and Kosten phenomenological model [38]:

$$\boldsymbol{\nabla} \cdot p + \frac{\rho_0 k_s}{\varphi} \frac{\partial \boldsymbol{v}}{\partial t} + R\boldsymbol{v} = \boldsymbol{0}, \tag{3}$$

$$\frac{\partial p}{\partial t} + \frac{\rho_0}{\varphi} \frac{c_0^2}{k_s} \boldsymbol{\nabla} \cdot \boldsymbol{v} = 0, \tag{4}$$

In Eqs. (3) and (4), R is the flow resistivity of the porous medium, φ its porosity and k_s the structure factor. These equations describe sound propagation in a porous rigid-frame medium.

The finite-difference time-domain (FDTD) method is used to solve Eqs. (1)–(4). The efficient staggered-in-time and staggered-in-space discretisation approach is chosen [39]. The advantages of this numerical scheme were described elsewhere [39]. Implementing the Zwikker and Kosten model does not induce additional difficulties compared to Eqs. (1) and (2) [20,40]. The validity of this model to simulate the interaction between sound waves and different types of outdoor soils has been discussed in Ref. [41].

Rigid surfaces are easily modeled by setting the normal component of the particle velocity to zero. Tree barks are modeled as a frequency-independent real-valued surface impedance as shown in [42]. The validity of this simplification is discussed in Section 3.4.

The FDTD method has been validated by comparison with measurements, analytical solutions and other numerical methods, over a wide range of acoustical applications [43,20,44,45].

3. Simulation parameters

3.1. Basic FDTD parameters

The spatial discretisation step is chosen to be 0.02 m, which is a compromise between limiting the computational cost and sufficiently capturing the road traffic noise frequency range. This means that calculations can be performed up to 1700 Hz (with a sound speed of 340 m/s), when demanding that at least 10 computational cells per wavelength are needed for accuracy reasons. A staggered, cubic spatial discretisation grid is used. The temporal discretisation step is taken so that the Courant number equals 1, leading to minimal phase errors, numerical stability and minimum computing times [39].

3.2. Simulation setup

An overview of the grid setup with dimensions is shown in Fig. 1. A line source at a height of 0.3 m (typical engine noise source height for light vehicles following the Harmonoise/Imagine road traffic source power model [46]) is placed above a rigid plane. A rigid plane is representative for a road surface top layer like concrete. Sound propagation in the soil layer itself (with a thickness of 0.5 m) is included in the simulation domain. A receiver plane is placed at 19 m from the source. A zone of 15 m in between the source and the receiver plane will be used to investigate the effect of various planting schemes. Perfectly matched layers are used to simulate an unbounded atmosphere at the left, right and upper boundary. Rigid planes are applied at $x=0$ and w_{rs} to model periodic extension of both the line source and the planting scheme considered. The width of the representative strip w_{rs} that is modeled depends on the chosen planting scheme, and is at
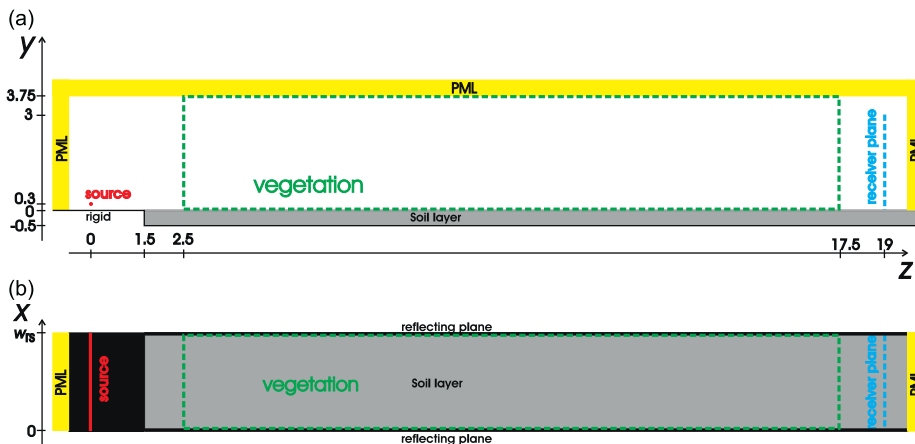

Fig. 1. Basic 3D grid setup ((a) cross-section and (b) plan view), showing the zone reserved for the evaluation of a specific planting scheme, the location of the line source and receiver plane, and the location of the perfectly matched layers (PML). The distance between the two mirror planes is indicted by w_{rs} and depends on the planting scheme.

minimum 1 m and at maximum 3 m. The validity of the mirror plane approach is checked by the 2D numerical example in Appendix A.

3.3. Soil parameters

In Ref. [41], reasonably accurate fits to measurements were found using the Zwikker and Kosten phenomenological model in case of sound propagation over forest floor and over grass-covered land. For these types of soil, very similar errors were found when using the slit-pore frequency-impedance model. For grass-covered ground, 26 sites were considered in Ref [41], ranging from "lawns" to "pastures". Based on these data, an (effective) flow resistivity of 300 kPa s m^{-2} and a porosity of 0.75 have been used to represent grassland in the current calculations. Measurements of the ground effect at pine stands and beech forests were considered as well in Ref. [41]. A flow resistivity of 20 kPa s m^{-2} and a porosity of 0.5 have been used to simulate the soil appearing under vegetation. The relation between porosity and tortuosity as described in Ref. [41] is applied.

Note that the main interest in these simulations is modeling reflection from a typical soil as found under vegetation. When there is interest in predicting the attenuation inside the porous medium itself, for the specific case of high sound frequencies and low flow resistivities, adaptations to the Zwikker and Kosten model should be made as proposed, e.g. in Ref. [47].

In this numerical study, the influence of a specific tree stand (tree species, tree spacing, presence of shrubs, etc.) on soil properties is not considered.

3.4. Acoustical properties of tree bark

Sound absorption of tree bark was studied by Reethof et al. [42] in an impedance tube (normal incident sound waves). Samples of the bark of species like *Quercus*, *Tsuga*, *Pinus*, *Fagus*, and *Carya* were considered. The absorption coefficients were mainly between 0.05 and 0.10 for sound frequencies between 400 Hz and 1600 Hz. For most species, effects were rather frequency independent in this range. Some species like *Carya* (Mockernut) gave significant higher absorption values, ranging up to 0.25 at 1.6 kHz. Based on these findings, an average frequency-independent value of 0.075 (normal incidence) can be justified for modeling reflection on the tree barks. This leads to a real-valued impedance of 51 times the impedance of air.

3.5. Planting schemes

In this study, four different tree planting schemes are considered, namely a simple cubic scheme (SC), a simple rectangular (SR) scheme, a face-centered cubic scheme (FCC) and a triangular scheme (T). The basic parameter to represent a certain scheme is the minimum distance between adjacent tree stem axes. This minimum distance is indicated by d in the SC, FCC and T scheme, and by d_1 (parallel to the road axis) and d_2 (normal to the road axis) in the SR scheme. In this representation, the SC and FCC have the same tree density per unit area ($=1/d^2$), while the planting scheme T is somewhat more dense (factor $2/\sqrt{3}$). The SR schemes have a tree density of $1/(d_1 d_2)$.

In Fig. 2, a representative strip is shown for each grid element. In case of a SC or SR scheme, such a strip is symmetric. In case of a FCC and T scheme, the computational cost can be further reduced by considering an asymmetric strip, cutting the stems at the borders in two.
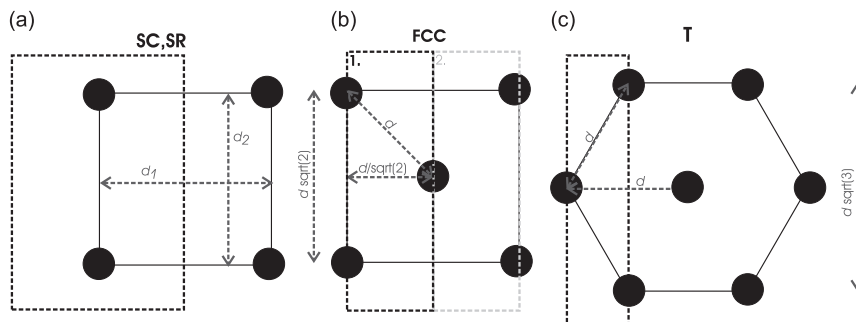

Fig. 2. Simple cubic (SC, $d_1=d_2=d$) (a), simple rectangular (SR, characterized by d_1 and d_2) (a), face-centered cubic (characterized by its minimum distance d between stems) (b), and triangular scheme (characterized by its minimum distance d between stems) (c). The representative strip is bordered by the dashed rectangles.

4. Approximation for small scattering elements

Explicitly modeling each element in vegetation imposes difficulties, especially in a volume discretisation technique employing a uniform grid as FDTD. The smallest structure that can be easily modeled is the computational cell. A meaningful representation of a small twig is usually not possible in a 3D grid without using techniques as grid refinement, conformal grids or subgrid-scale modeling which in all cases leads to more complex calculation schemes and a higher computational cost. A valuable approach is subgrid-scale modeling [48], as illustrated by means of the pseudo-spectral time-domain (PSTD) model where scattering was modeled near a small tree based on a detailed geometrical representation of it [49]. A main problem with using full geometrical details is access to such data, and the loss of the naturally occurring variation in such structures. Therefore, a more practical and easy-to-apply approach is proposed here. It is based on a statistical spatial distribution of (basic) filled grid cells, imitating the interaction between vegetation structures and sound waves, while preserving the inherent randomness. Besides modeling of multiple scattering and a high portion of transmission through the vegetation, the effect of absorption by branches and twigs can be included by making these filled cells partly absorbing. Focus is on scattering by woody material. Important interactions between leafs and sound waves are expected to occur at sound frequencies beyond the range that is modeled here [19], and is considered to be of limited importance when looking at total A-weighted road traffic noise [37].

4.1. Low growing vegetation and shrubs

Firstly, this approach will be used to model the interaction between sound and shrubs and other low, ground-covering vegetation. Near full ground cover is possible for many species or combinations of species. As a result, a uniform distribution of scatterers will be assumed. The above-ground woody biomass volume taken by the shrubs is then evenly distributed over the artificial scatterering cells in FDTD. Given the absence of more detailed data on the acoustic surface properties of the branches and twigs for this type of vegetation, the same data as for tree bark is used (see Section 3.4). The addition of (some) absorption will not only account for the interaction between the surface of plant material and acoustic waves, but also for damping by sound-induced vibration of plant elements.

For the FDTD calculations, the input parameter in the above described approach is 1 minus the porosity of the shrubs, which equals the chance of making a grid cell a scattering cell. Information on this parameter is not directly available in relevant literature. The basic parameter that is found is the above-ground total dry biomass per unit area. In combination with typical shrub height, mass distribution over leafs and woody parts, mass density of dry wood in shrubs, and the typical water content of woody parts, the above-ground shrub porosity can be estimated.

A wide range of values for above-ground (oven-dried) total biomass per unit area can be found in literature. The measurements in Ref. [50] for different shrub type ecosystems reported values from 0.5 to 2 kg/m^2, for shrubs heights lower than 1.5 m and ground coverage ranging from 42 percent to 97 percent. Furthermore, an overview is given in [50] for some Mediterranean species, showing values in the range from 1 kg/m^2 to 6.68 kg/m^2, for shrub heights ranging from 1 m to 4.5 m. The average value for low trees and shrubs (12 species) reported by Harrington [51] was 5.4 kg/m^2. Navar et al. [52] found an average of above-ground total biomass per unit area of 4.44 kg/m^2. Top heights of the various species involved in the latter ranged from 1.9 m to 5 m.

The distribution of biomass over leafs, branches and stems was measured to be 5.6 percent, 61.5 percent, and 32.8 percent, respectively, in Ref. [52]. Measured values for the ratio leafs to total above-ground biomass ranged between 3 percent and 34 percent, with a median at 18 percent as reported in Ref. [51]. Navarro-Cerrillo and Blanco-Oyonarte [50] give an overview of photosynthetic-to-total phytomass values for many species; most of the data fell in the range between 12 percent and 19 percent.

The water content and water distribution between woody biomass and leafs depend on many variables like plant segment, stand location, age, etc. [53]. The water content in the woody parts was found to be typically 40 percent according to the measurements in [53]. This is consistent with the typical range of water content of leafs in deciduous shrubs ranging from 50 percent (older full-size leafs) to 65 percent (lush new leafs) according to Ref. [54]. In Ref. [53], measurements showed values between 50 percent and 60 percent.

Mass density of (dry) wood in shrubs falls in the range from 400 to 1100 kg/m^3 [55]. These values depend largely on shrub species. The median value on this data is close to 650 kg/m^3.

The in-situ shrub porosity φ_{shrubs} of woody plant elements can then be calculated as follows:

$$\varphi_{shrubs} = 1 - \frac{m_{tot,dry}}{H_{shrubs}} \left[\frac{f_{wood,dry}}{\rho_{wood,dry}} + \frac{f_{wood,dry}}{\rho_{water}} \left(\frac{w_{wood}}{1-w_{wood}} \right) \right], \tag{5}$$

with $m_{tot,dry}$ the total, dry above-ground biomass (in kg/m^2), H_{shrubs} the average height of the shrubs (in m), $f_{wood,dry}$ the mass fraction taken by the dry wood, $\rho_{wood,dry}$ the mass density of dry wood (in kg/m^3), ρ_{water} the mass density of water, and w_{wood} the fraction of water present in woody parts of the shrubs in-situ. When using typical values from the literature review as discussed above ($m_{tot,dry}=4$ kg/m^2, $f_{wood,dry}=0.9$, $\rho_{wood,dry}=650$ kg/m^3, $\rho_{water}=1000$ kg/m^3, $w_{wood}=0.4$) and by taking $H_{shrubs}=1$ m, this leads to an in-situ shrub porosity of near 0.99, meaning that 1 percent of the volume is taken in-situ by water-containing woody plant material. Values of 0.98 and 0.995 are modeled as well to study the range of

possible effects given the use of default values only. Note that such values could be representative for many combinations of the above described parameters.

4.2. Scattering from tree crowns

Including tree crowns is mainly intended to estimate the negative effect of downward scattering in the simulations. The tree crown is – in a first approximation – represented by a sphere. The upper half of this sphere is neglected to limit the computational domain in the *y*-direction. The use of small, scattering elements is applied here as well. It is assumed that near the center of the crown, most woody material is present leading to a higher chance of filling a given computational cell. Such a larger chance will lead to clustering of filled grid cells, which could be representative for bigger structures in the crown like a prolongation of the stem, or bigger branches. At the surface of the sphere representing the tree crown, a very small change that a grid cell becomes a scattering cell is applied. Note that since the frequency content in the current simulations is limited to 1700 Hz, effects by the presence of leafs will be rather limited and this effect is neglected. Since the exact distribution of biomass in a tree crown is not known, various approaches were tested as regards the distribution of scattering elements to have an idea on the sensitivity of the conclusions on such choices.

5. 3D numerical calculations

The 3D numerical results are depicted in different ways in the remainder of this paper. In a first representation, (total) traffic noise insertion loss values (in dBA) are linearly averaged over all receivers in the plane at $z=19$ m and shown by means of bar plots. A light vehicle (vehicle type 1 following the Harmonoise/Imagine road traffic source model, representative for a passenger car) at a vehicle speed of 70 km/h is modeled. Separate bars are shown for receiver heights ranging from ground level up to 3 m, and for receiver heights from 1 to 2 m (height of human ear for both children and adults). Averaging over a range of receivers summarizes results. As a reference, the same type of ground has been used (although hypothetical, the typical soft ground only develops under vegetation). In this way, the effect of the ground is singled out, and the effect of the presence of the stems and vegetation only is assessed. An alternative reference situation is sound propagation over grassland. As discussed in Section 1, these results give a global estimate of what can be expected when replacing an existing piece of grassland by a vegetation belt. Furthermore, insertion loss spectra are shown at a single receiver height along the representative strip, or as (linearly) averaged results over the receiver plane in function of vehicle speed in case of a more detailed analysis.

A single source at a height of 0.3 m is considered (following the Harmonoise/Imagine road traffic source model), and both the engine and rolling noise source power is assigned to that source height. The effect of also considering sound propagation from a source at a height of 0.01 m, relative to the road surface, was shown to be limited in the current setup and averaging approach (see Appendix B). Unless otherwise stated, the stems have a length of 2.5 m, stem diameters are constant in the tree belt, and the full area assigned for vegetation as shown in Fig. 1 is used. The acoustic effects of the various layers in the vegetation belt (shrub zone, stem zone, and crown zone) are considered separately to study their individual effect, unless stated otherwise. Furthermore, a coherent line source is modeled. In Appendix C, the effect of source type (coherent versus incoherent line source) is studied for some configurations. An overview of the 3D simulations performed can be found in Tables D1 and D2 in Appendix D.

5.1. Effect of soil

The effect of the presence of a typical soil as found under vegetation is compared to sound propagation over grassland, for total traffic noise (light vehicles) at different vehicle speeds in Fig. 3. With increasing height above the ground surface, the effect of a different soil becomes less pronounced. Traffic noise insertion losses at low vehicle speeds are dominated by
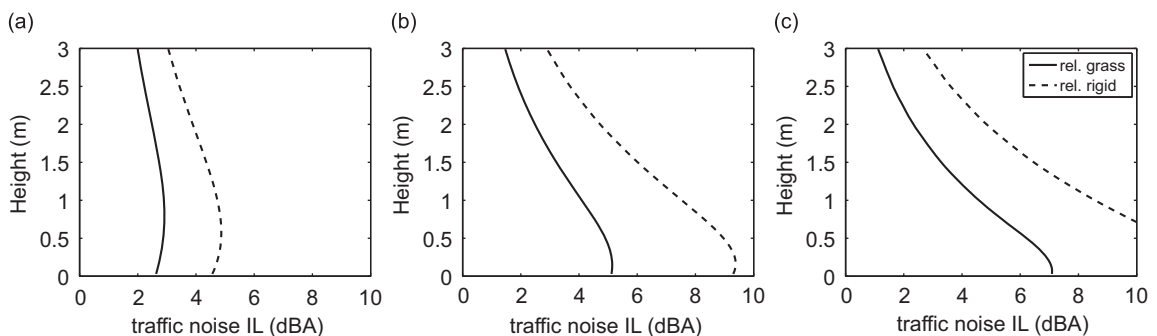

Fig. 3. Traffic noise insertion loss with height for various vehicle speeds ((a) 30 km/h, (b) 70 km/h, and (c) 110 km/h), in case of sound propagation over uncovered vegetation soil. Results are referenced to sound propagation over grass-covered and rigid ground.

low frequencies and lead to less variation with height. Measurements of sound propagating over acoustically soft ground from a source at limited height show similar behavior [56]. Close to the ground, differences between the two types of soils at the higher vehicle speeds may exceed 7 dBA. The average effect for a vehicle speed of 70 km/h equals 3.3 dBA (with a standard deviation of 1.2 dBA) for receivers between $y=0$ m and 3 m, and 3.2 dBA (standard deviation of 0.5 dBA) for receivers between $y=1$ m and 2 m. For comparison, results are also referenced to sound propagation over a rigid ground in Fig. 3, showing a large decrease in traffic noise insertion loss.

5.2. Analysis of band gap effects

In this section, the presence of band gap effects is examined for both 2D and 3D calculations for the SR 1 m/2 m scheme, for cylinders/tree stems with diameters of 22 and 44 cm. In the first case, a coherent plane wave and infinitely long cylinders are modeled in absence of a ground plane (and referenced to free field sound propagation). In the second case, a coherent line source is modeled and 2.5 m-high stems above an absorbing ground (and referenced to sound propagation over the same ground in absence of stems). Both fully rigid stems and partly absorbing stems are considered. Results are represented as 1/9 octave bands to have a more detailed look at the insertion loss spectrum. For each receiver position, the insertion loss is calculated. Next, the insertion losses over all receiver positions are linearly averaged. A receiver height of 2 m is considered in case of the 3D simulations.

The lowest-order insertion loss peaks at 85 Hz and 170 Hz in Figs. 4 and 5 correspond to interference of scattered waves for inter-stems distances of 2 m normal to the road (for a speed of sound equal to 340 m/s). These peaks correspond to Bragg's law for normal incident waves. It can be observed that such peaks are more pronounced for plane wave sound propagation than for sound propagation over an absorbing ground surface, which is consistent with findings in [36]. At these low frequencies, only the 44-cm diameter stems provide a sufficient amount of scattering. For the 22-cm diameter stems, only a very small insertion loss is observed at these same frequencies. For the latter, higher order band gaps will make the more important contributions to overall IL. Modeling an incoherent line source does not seem to affect the frequency and magnitude of these peaks (not shown). Further analysis confirms that mainly the spacing normal to the road determines at what frequencies insertion loss peaks are found. On the other hand, decreasing the spacing along the road increases the magnitude of the insertion loss peaks due to the increased filling fraction. A sufficient amount of back scattering is needed, given the limited depth of the vegetation area considered. As an example, a SR 2 m/3 m 44 cm gives similar low-frequency insertion loss peaks as SR 1 m/3 m 44 cm (easy-to-identify peaks are situated at 57 Hz, 113 Hz, 170 Hz, 227 Hz), but the magnitude of these is more pronounced with a spacing along the road of 1 m (not shown).

At higher frequencies, both interference corresponding to higher-order harmonics of the basic lattice spacing, and direct shielding by the tree stems is observed, yielding complex insertion loss spectra. At very low frequencies, uniformity over the modeled strip is observed. At higher frequencies, on the other hand, there is significantly more variation in insertion loss along the representative strip, clearly shown by the larger values for the standard deviation: The exact location relative to the position of the stems plays a more important role.

Including the absorption characteristics of tree bark seems to broaden the low-frequency peaks to a limited extent. At higher frequencies, including absorption increases the insertion loss relative to the rigid stems, although frequency independent impedances are modeled at the surfaces. While the 2D insertion loss values are positive over the full
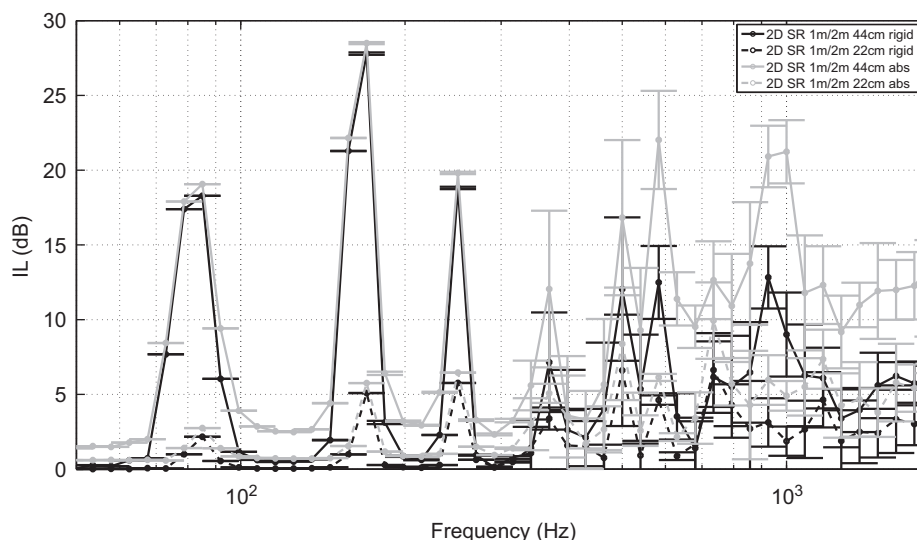

Fig. 4. Plane wave IL spectra for SR 1 m/2 m schemes, averaged over the width of the representative strip, for stem diameters of 22 cm and 44 cm, and for rigid and partly absorbing stems. The error bars have a total length of two times the standard deviation. The reference is free field sound propagation.
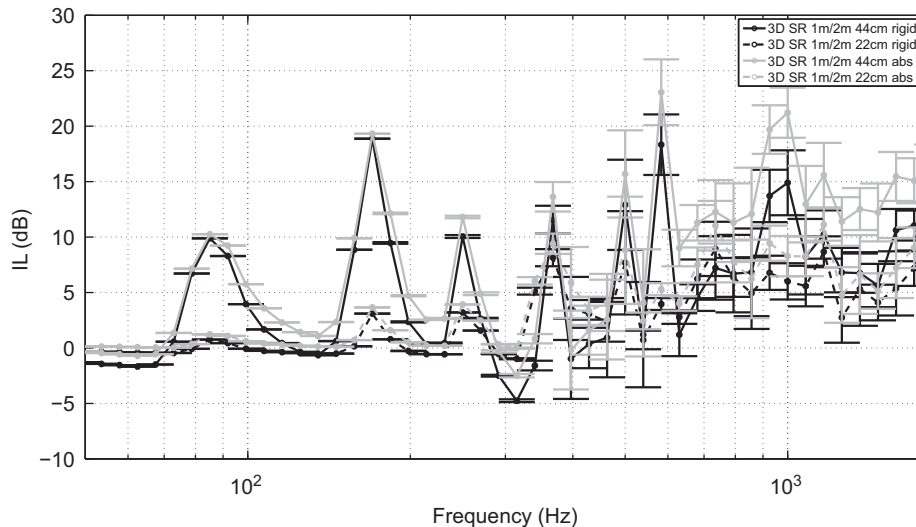
Fig. 5. Line source IL spectra for SR 1 m/2 m schemes, averaged over the width of the representative strip at a height of 2 m above vegetation soil, for a stem diameter of 22 cm and 44 cm, and for rigid and partly absorbing stems. The error bars have a total length of two times the standard deviation. The reference is sound propagation over the same soil in absence of stems.

frequency range considered, an increase in the sound level is observed near 300 Hz for the 3D case and rigid stems. Such negative effects are somewhat less pronounced when applying typical absorption values for tree bark.

It can be concluded that the presence of the typical soil appearing under vegetation, or source representation (coherent line source, incoherent line source, or plane wave) does not affect the possibility to exploit periodicity. Tackling engine noise (near 100 Hz) by using the periodicity in tree belts seems difficult. Large stem diameters are needed to yield a sufficient amount of scattered energy at these low frequencies. Furthermore, this condition is enhanced since in case of a larger spacing a sufficient filling fraction still has to be obtained. For practical combinations of tree stem diameter and tree spacing (see discussion in Section 6), pronounced band gap effects will therefore be mainly expected in case of limited spacings (e.g. SC 1 m 11 cm), so at frequencies where we can also expect direct shielding effects.

5.3. Effect of stem diameter and planting scheme

The effect of the tree diameter and the choice of the planting scheme become clear from Fig. 6. Three stem diameters were considered, namely 11 cm, 22 cm, and 44 cm, and for a passenger car at a vehicle speed of 70 km/h. The simulation results at vehicle speeds of 30 km/h and 110 km/h can be found in Table D1. Many of the planting schemes with the 44 cm tree diameters, and some of the 22 cm tree diameters, will be hard to achieve in practice, but were retained as they allow a better evaluation of the importance of some parameters. Remarks on practical aspects can be found in Section 6.

With increasing tree stem diameter, traffic noise insertion loss is more pronounced for each planting scheme considered. Furthermore, with increasing distance between the stems, traffic noise insertion loss becomes smaller and the importance of the stem diameter decreases, illustrated by the decreasing slopes in Fig. 6.

The FCC 2 m, T 2 m and SC 2 m have the same minimum planting distance and can therefore be compared. For the 11-cm and 22-cm diameter stems, the effect of the scheme considered is unimportant. For the 44-cm diameter stems, there is a light preference for T upon FCC and SC.

For the SR schemes, the orientation relative to the road axis is important. Although the filling fraction for SR 1 m/2 m is much smaller than for SC 1 m, effects are more or less similar for the modeled diameters of 22 cm and 44 cm. At a vehicle speed of 70 km/h, SR 1 m/2 m becomes even better than SC 1 m for a stem diameter of 44 cm. Similarly, SR 2 m/3 m shows a behavior that is much closer to SC 2 m than to the average between SC 2 m and SC 3 m for 22-cm and 44-cm diameter stems. On the other hand, SR 2 m/1 m (i.e. scheme SR 1 m/2 m rotated over 90°) gives a traffic noise shielding equivalent to SC 2 m for the 22 cm and 44 cm stem diameters. This means that SR 1 m/2 m clearly outperforms SR 2 m/1 m. It seems that the spacing, parallel to the road is the main parameter to predict road traffic noise shielding. For the low diameter of 11 cm, SR 1 m/2 m is very close to the average between SC 1 m and SC 2 m. The same holds for SR 2 m/3 m, which is the average of SC 2 m and SC 3 m. Furthermore, the acoustic behavior of SR 2 m/1 m is equivalent to SR 1 m/2 m, and SR 2 m/3 m is equivalent to SR 3 m/2 m for low stem diameters.

The reason for this behavior is that the spacing parallel to the road axis should be limited to provide sufficient scattering in case of a line source. This is needed to prevent sound arrival at the receiver without interacting with the trees, and to have a sufficiently scattered sound field in the first rows to be able to exploit periodicity, as discussed in Section 5.2.
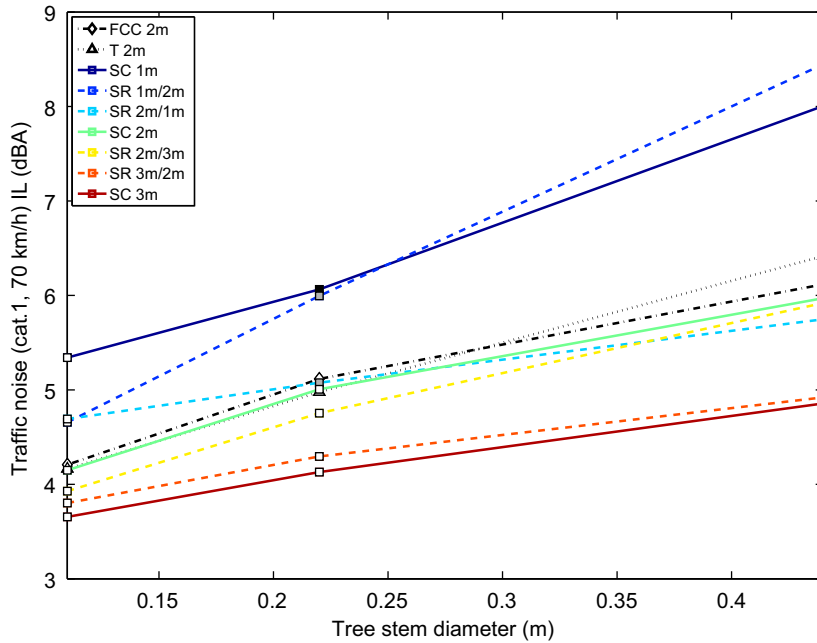
Fig. 6. Average traffic noise IL (for a light vehicle at 70 km/h) in the receiver plane, in function of tree stem diameter, referenced to sound propagation over grassland (receiver heights from 1 to 2 m). Different schemes were considered. The filling of the markers indicate whether the planting scheme is realistic with ordinary tree plantings (white), if special measures needs to be taken (gray), or if the planting scheme will be hard to realize (black). See Section 6 for discussion on this topic.
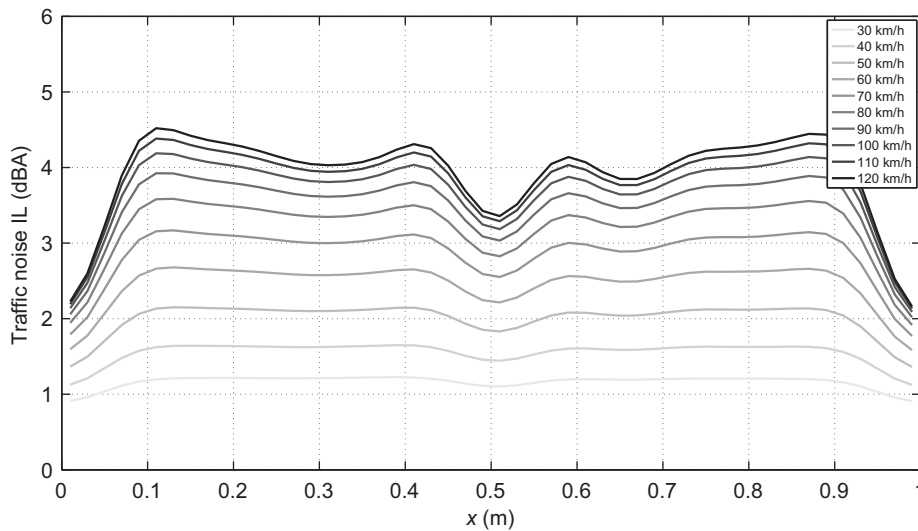
Fig. 7. Traffic noise IL (dBA) along a representative part of planting scheme SR 1 m/2 m 22cm (at $y=2$ m), for light vehicles at speeds ranging from 30 to 120 km/h. The reference situation is sound propagation over vegetation soil.

The effect of vehicle speed can be illustrated by Fig. 7 for SR 1 m/2 m 22 cm. A receiver line at a height of $y=2$ m is considered, and the total traffic noise insertion loss over the modeled strip is shown with increasing vehicle speed. For the higher vehicle speeds, the effect of the planting scheme is clearly more pronounced. Above 100 km/h, the effect of vehicle speed becomes very small. While for the lower vehicle speeds a more uniform insertion loss is observed over the receiver line, for higher vehicle speeds there is more variation. At higher vehicle speeds direct shielding is more important, and the location along the receiver line, relative to the position of the trees, becomes relevant.

5.4. Effect of number of rows and stem height

In Fig. 8, the effect of the number of rows is considered for the SR 1 m/2 m scheme, for a tree stem diameter of 22 cm and 44 cm. An increasing number of tree stems were removed, starting from the receiver plane. The vegetation soil was replaced by grass-covered soil accordingly. In case of 2 rows, only close to the road trees are present. In case of 22-cm diameter trees, a near-linear behavior is found when increasing the number of rows of trees, referenced to an identical soil without trees. In case of a diameter of 44 cm, a large improvement is observed when going from 0 to 2 rows, which then becomes linear when further increasing the number of rows.

With increasing tree height, the traffic noise shielding increases. However, the effect of stem height is rather unimportant, once a height of 1 m is reached. Averaged over receiver heights from ground surface to 3 m, a difference of about 1 dBA is observed for a stem height of 1 m high compared to 2.5 m, and for a stem diameter of 22 cm. Even low stems perform well due to the presence of a source close to the vegetation area and close to the ground surface. Note that tree crowns were absent when evaluating the importance of number of rows and stem height. The presence of crowns below or at receiver height could be beneficial, compared to scattering from crowns above the receiver height (see Section 1).

5.5. Effect of crown scattering

Since the exact distribution of biomass in a tree crown is not known, various approaches were tested as regards the distribution of scattering elements to estimate the sensitivity of results on this choice. In the first 3 approaches, a 3rd order power-law is used to relate the probability of filling a cell in function of the normalized distance towards the stem-axis. The maximum probabilities at the stem axis are 0.5 (approach 1), 0.33 (approach 2) and 0.2 (approach 3). Next, a 5th order (approach 4) and 7th order (approach 5) power law is applied, for a maximum probability of 0.5 at the stem axis. The minimum probability at the sphere surface is 0.01 in all representations. Calculations are made for the lower half of spherical tree crowns, starting at a height of 2.5 m, in absence of stems, above vegetation soil. Crowns organized as a SR 2 m setup are considered.

Scattering from tree crowns leads to an increase in sound pressure level and consequently a decrease in insertion loss. The calculated insertion loss values, (linearly) averaged over the receiver plane at heights between 1 m and 2 m, are -0.8, -0.5, -0.3, -0.6 and -0.4 dBA for approaches 1–5 (lower half of the tree crown only). It was numerically tested for approach 1 that also including the upper half of the crown results in 0.2 dBA additional scattering.
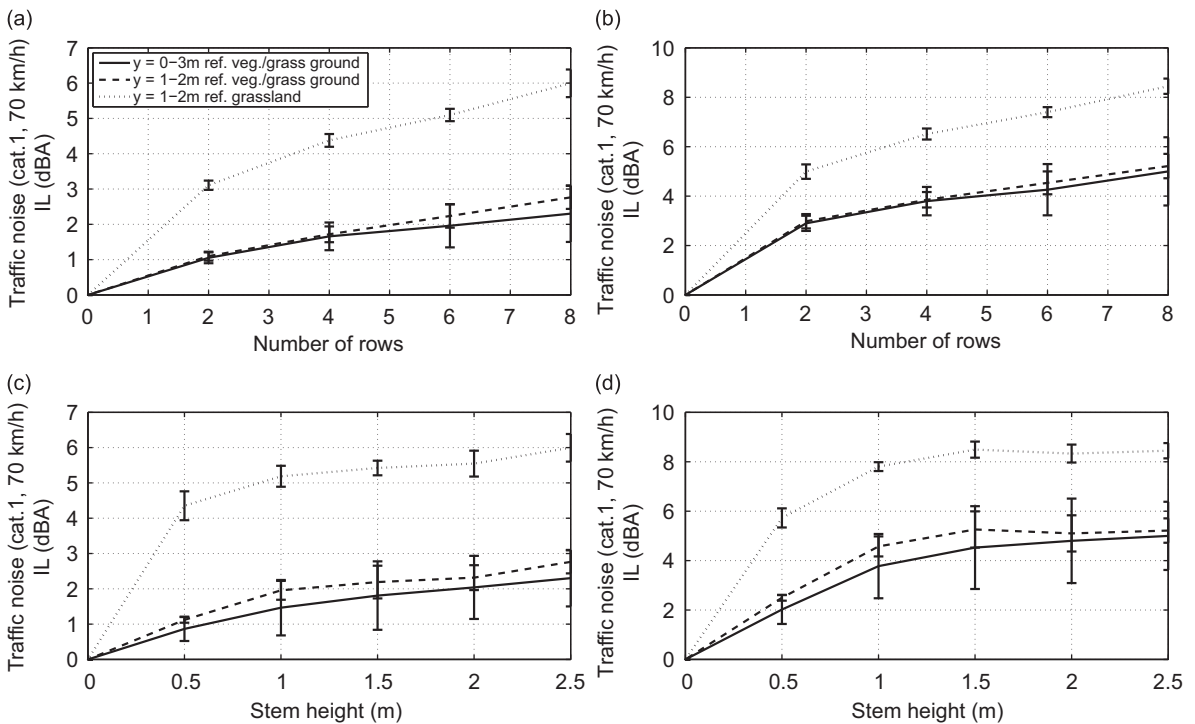
Fig. 8. Total traffic noise IL for a light vehicle at 70 km/h, averaged over the receiver plane, in function of number of rows ((a) and (b)) and stem height ((c) and (d)). Results are referenced to sound propagation over vegetation soil (at heights between 0 and 3 m, and at heights between 1 and 2 m), and to sound propagation over grassland (at heights between 1 and 2 m). The total length of the error bars equals two times the standard deviation. In (a) and (c), planting scheme SR 1 m/2 m 22 cm is considered; in (b) and (d) planting scheme SR 1 m/2 m 44 cm.

Measurements of sound scattering by tree crowns behind a highway noise barrier (in a still atmosphere) [19] fall within the range of the values predicted here. Simultaneous measurements were performed behind part of the noise barrier with and without a (single) row of trees behind it. A log-linear relationship between sound frequency and level difference between these two locations was measured (from $+0$ dB at 1 kHz to $+5$ dB at 10 kHz because of the crowns). When applied to a light vehicle road traffic power spectrum at 70 km/h, this leads to an insertion loss value (of the tree crowns) of -0.8 dBA. It can be concluded that the global effect of crown scattering is in qualitative agreement with measurements, although scattering by leafs is not specifically addressed in the proposed numerical model.

5.6. Effect of shrubs

Two approaches were followed for comparing the effect of the presence of shrubs. First, the same amount of above-ground biomass per unit area is modeled, distributed over shrubs with a height of 0.5 m, 1 m, 1.5 m and 2 m. This corresponds to shrub porosities of 98 percent, 99 percent, 99.33 percent and 99.50 percent, respectively. Secondly, two fixed shrub porosities were modeled, namely 99 percent and 99.5 percent. In the latter, the total amount of above-ground biomass increases with shrub height.

For an equal amount of biomass, there is a preference for dense low vegetation as shown in Fig. 9. The minimum performance that is observed for traffic noise shielding is for shrubs with a height near 1 m or 1.5 m, depending on the receiver height zone considered. For a 2-m high shrub with the same amount of above-ground biomass, the traffic noise shielding increases again. Note that the standard deviation when considering receiver heights from 0 to 3 m can be quite high. More detailed analysis shows that for the more densely packed shrubs, positive effects for total traffic noise are mainly observed for receivers above the shrub height. Zones with negative effects, mainly for the higher vehicle speeds, were observed below the shrub height. For the 2-m high shrubs, such zones with negative effects do not appear.

For fixed shrub porosity, there is a preference for the 2-m high shrubs. For receiver heights between 1 m and 2 m, the difference between 0.5 m, 1 m and 1.5 m shrubs is very similar, although there is 3 times as much vegetation mass for the 1.5-m shrubs compared to the 0.5-m shrubs.

A 2-m high shrub zone with a length of 15 m, for total above-ground dry biomass of 4 kg/m², gives an average traffic noise insertion loss of 4.7 dBA for a light vehicle at 70 km/h at typical ear heights (relative to sound propagation over grassland). The positive effect of the presence of the ground is included here, accounting for 3.2 dBA. The effect of a soft ground (developed by the presence of the shrubs) is therefore the major contribution to the traffic noise shielding.

Effects of different random realizations of the shrub layer are very minor (<0.1 dBA) when considering averaged results over the receiver planes for total traffic noise insertion loss.

5.7. Combining shrubs, crown scattering and the presence of stems

In this section, the acoustical effect of combinations of low (understorey) vegetation, crown scattering, and the presence of stems are shown. Crown scattering approach 1 is applied. Shrubs of 0.5 m high with a porosity of 98 percent

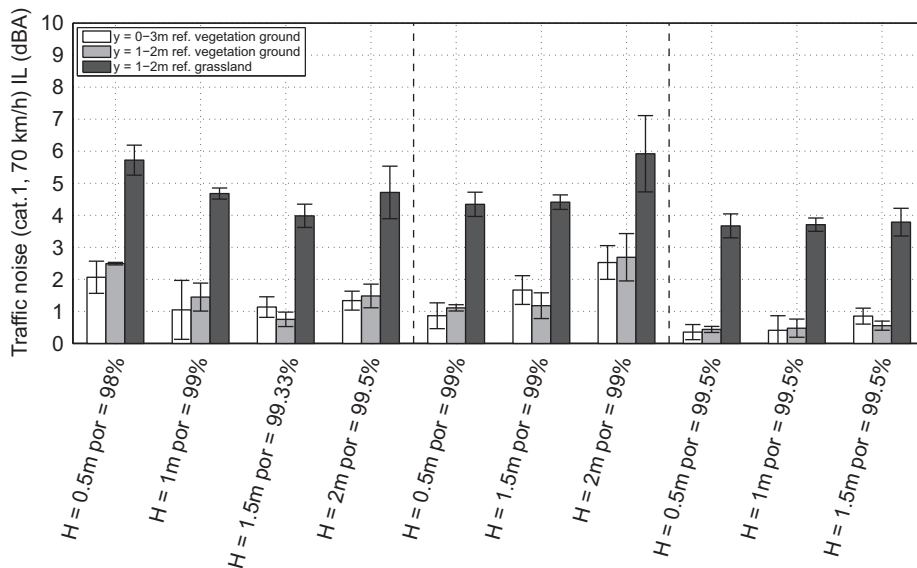**Fig. 9.** Total traffic noise IL for a light vehicle at 70 km/h, averaged over the receiver plane, for shrubs above vegetation soil. Results are referenced to sound propagation over vegetation soil (at heights between 0 and 3 m, and at heights between 1 and 2 m), and to sound propagation over grassland (at heights between 1 and 2 m). The total length of the error bars equals two times the standard deviation.
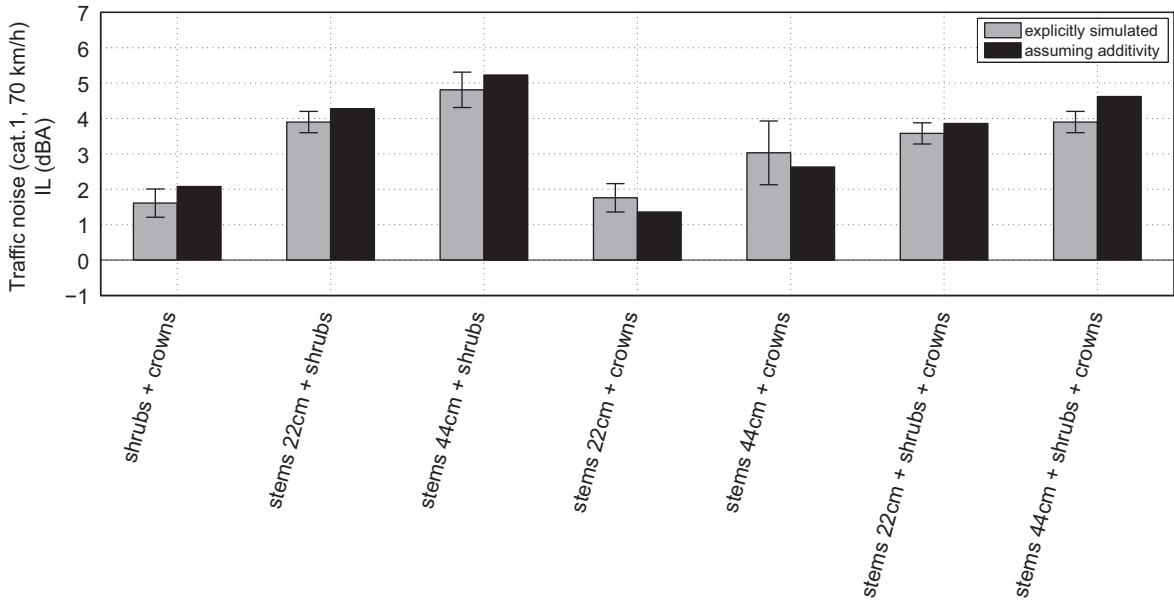
Fig. 10. Total traffic noise IL for a light vehicle at 70 km/h, averaged over the receiver plane, for combinations of shrubs (H=0.5 m, por=0.98), stems (SC 2 m 22 cm and SC 2 m 44 cm), and tree crowns (approach 1) above vegetation soil. Explicitly simulated combinations are compared to the result of adding the insertion losses of single effects. Results are referenced to sound propagation over vegetation soil (at heights between 1 and 2 m). The total length of the error bars equals two times the standard deviation.

are used. SC 2 m tree planting schemes are applied, with diameters of 22 cm and 44 cm. Identical realizations are used for the crowns and low vegetation in the different combinations.

In Fig. 10, explicitly modeled combinations are shown and compared to the result of adding the insertion losses of single effects (i.e. stems only with a diameter of 22 cm or 44 cm, shrubs only, and tree crowns only). Effects of stems, crown scattering and low vegetation can be considered as more or less additive based on these simulations, when considering sound propagation referenced to the same type of soil. Adding insertion losses of separate effects, and comparing the results to explicitly modeling combinations, yield differences of at most 0.7 dBA (averaged over receiver heights from 1 to 2 m). It is clear that additivity does not hold when referenced to sound propagation over grassland, since the positive ground effect is included in all parts. These findings show that the different parts in vegetation belts only interact to a limited extent when considering typical road traffic noise spectra. As a result, it does not seem necessary to perform simulations of combinations of understorey vegetation, different stem schemes and crown representations to have an adequate estimate of the global effect.

This additivity of scattering by vegetation and the sound–soil interaction is consistent with the findings in Refs. [1,31], and could potentially lead to simplified and less computationally intensive approaches than the one used in this study.

Note that the shrub mass density per unit area assumed here exceeds what would be practically possible as an understorey in a (dense) tree stand. However, the main purpose of this section was checking possible interactions between the different layers in a vegetation belt.

5.8. Randomization and lattice defects

The presence of (some) randomness in the stem center location and stem diameter will be inherent in practical realizations of tree belts. Secondly, sonic crystal research showed that positive effects could be expected by inducing lattice defects in case of densely packed cylinders, leading to a broadening of insertion loss peaks [34]. Since road traffic noise spectra are characterized by a broad frequency range, this effect is worth studying.

The use of the reflecting plane approach as applied in this numerical study can only lead to periodic planting schemes along the road axis. Only the effect of random shifts orthogonal to the road can be studied.

5.8.1. Shifts in stem center location

In a first step, the effect of random shifts in stem center location is studied for some schemes with a spacing of 2 m normal to the road. It is clear that complete randomness is not of practical use, since it conflicts with the minimum planting distance needed for development of neighboring trees. Random shifts up to 0.75 m were allowed normal to the road and in both directions, compared to a constant spacing. Three random realizations are considered in each case and the insertion losses were linearly averaged afterwards.

Inducing some (pseudo)randomness in the location of the stem center is predicted not to decrease traffic noise insertion loss as illustrated in Fig. 11. In the more densely packed SR 1 m/2 m 44 cm scheme, an increase in traffic noise insertion loss near 0.5 dBA is observed. For the SC 2 m scheme, the additional positive effect of randomness in stem center location is very limited.

5.8.2. Randomness in tree diameter

In a SR 1 m/2 m scheme, random variations in tree stem diameter are modeled, ranging from 22 cm to 44 cm, following a uniform distribution. The (linearly) averaged traffic noise insertion loss of 3 such realizations (referenced to vegetation soil, for receivers between 0 and 3 m) shows a noise reducing potential (3.9 dBA) that is closer to the performance of a uniform 44-cm diameter tree stand (5.0 dBA) than to the uniform 22-cm diameter tree stand (2.3 dBA). Similarly, for SC 2 m, mixing diameters lead to a traffic noise insertion loss of 2.1 dBA, which is again closer to the uniform 44-cm diameter tree stand (2.5 dBA) than to the uniform 22-cm diameter stand (1.4 dBA). This shows that randomness in tree diameter is positive from the viewpoint of noise reduction. Selecting for identical trees should therefore not be encouraged.

5.8.3. Including gaps

The effect of omitting some rows for planting schemes SR 1 m/2 m is simulated, with fixed stem diameters of either 22 cm or 44 cm. Four different realizations of 2 missing rows were simulated and compared to using 8 rows to fill the zone designed for the planting scheme (see Fig. 12). Leaving out some rows does not significantly influence the averaged traffic noise insertion loss in the receiver plane. Some of such realizations including gaps seem to even improve noise shielding a
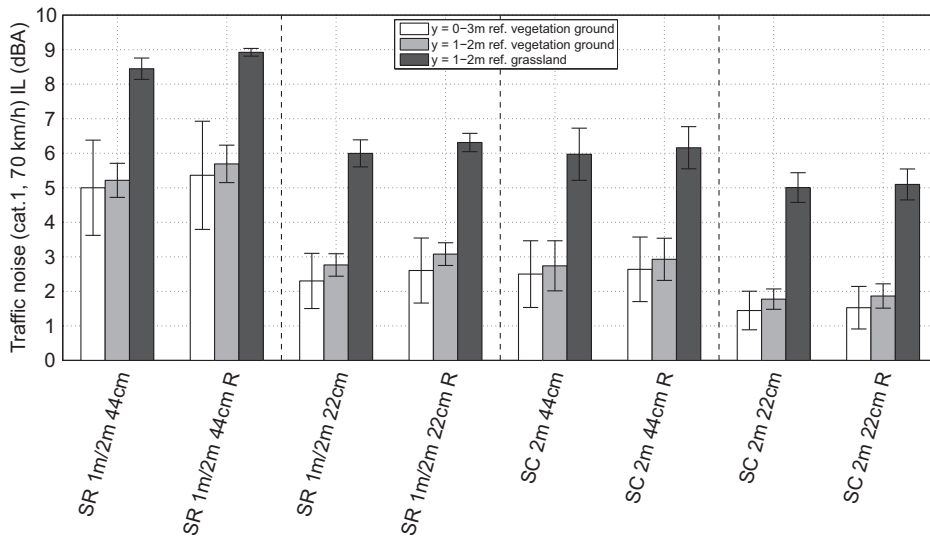
Fig. 11. Total traffic noise IL for a light vehicle at 70 km/h, averaged over the receiver plane, for different schemes, including random shifts in stem center location (indicated by "R"). Results are referenced to sound propagation over vegetation soil (at heights between 0 and 3 m, and at heights between 1 and 2 m), and to sound propagation over grassland (at heights between 1 and 2 m). The total length of the error bars equals two times the standard deviation.
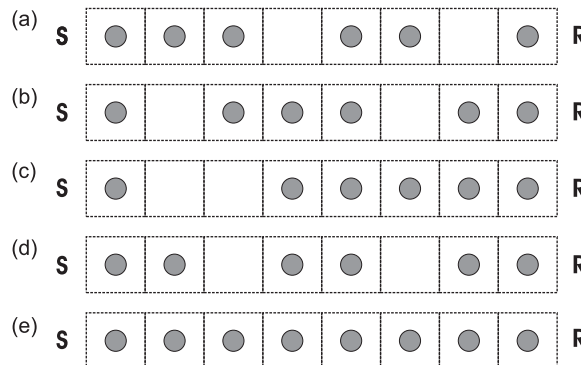
Fig. 12. The 4 realizations considered (shown as representative strips) in case of 2 missing rows out of 8 (a)–(d). The fully populated grid is shown in (e). S and R indicate the source and receiver side, respectively.

little (realizations *a* and *d*: $+0.2$ dBA) for the tree diameter of 44 cm (referenced to sound propagation over grassland, and receiver heights between 1 m and 2 m). For the 22-cm diameter stems, there is a small reduction (at maximum -0.3 dBA) in insertion loss. Similar conclusions could be drawn by considering SC 2 m. Omitting some rows in between the tree stand is better for noise shielding than, e.g. limiting two rows at the end, as shown in Fig. 8. It is assumed that near these open spaces, a vegetation soil is developed as well, which is not expected in case of limiting the tree belt to 6 consecutive rows. It is discussed in Section 6 that this finding is interesting for the practical realization of tree stands.

5.9. Sound propagation over rigid thin noise barrier

For comparison, the FDTD model applying mirror planes is used to calculate the insertion loss of a rigid rectangular screen with a thickness of 0.1 m, placed at 3 m relative to the source position. In this approach, the screen is infinitely long and parallel to the road axis. The screen is placed on grass-covered ground, and road traffic noise levels are referenced to sound propagation over unscreened grassland. The noise shielding by vegetation belts is referenced to grassland as well. Screen heights of 0.5 m, 1.0 m, 1.5 m, 2.0 m, and 2.5 m were considered. The insertion losses obtained (for receivers between 1 m and 2 m, and a vehicle speed of 70 km/h) are 3.6, 6.2, 8.8, 10.6, and 11.7 dBA, respectively. Some of the vegetation schemes that can be practically realized (see Section 6) could compete with a screen of 1 m or even 1.5 m. An important reason is the preservation and change of the ground effect when vegetation is used. In case of a classical screen, this positive ground effect can be (partly) lost by preventing the direct and ground-reflected wave to destructively interfere. Note that the screen calculations are performed for a coherent line source. Noise barrier shielding in case of an incoherent line source is expected to be lower [57,58] than the results shown here. This fortifies the conclusions drawn. Furthermore, classical noise barriers are sensitive to an important decrease in shielding in case of downwind sound propagation, even at short distance [59,60]. In case of a stand of vegetation, such negative effects are expected to a much lesser extent since vegetation acts as a windbreak; the strong vertical gradients in the horizontal component of the wind speed as observed near the barrier top [21] will not appear.

6. Practical considerations

Well-established empirical relationships exist between the number of trees per unit area and their stem diameter [61]. Based on such relationships, the suggested tree density–tree diameter combinations considered in this work are not all realistic in ordinary tree plantings, especially for the stems with a diameter of 44 cm. Such results are nevertheless kept in the analysis to reveal trends. Following findings in this study are interesting from the practical point of view.

Firstly, numerical simulations indicated that omitting some rows of trees does not affect the traffic noise insertion loss of the tree stand. Trees planted in densely clustered zones followed by open spaces could therefore be practically achievable, as this ensures that more resources (light, water and nutrients) are available for tree growth and that higher tree densities can be obtained.

Secondly, there is a preference for rectangular schemes, for stem diameters of 22 cm. The noise reduction obtained by scheme SR 2 m/3 m is close to the one of SC 2 m, although SR 2 m/3 m has a smaller tree density (0.17 m^{-2}) than SC 2 m (0.25 m^{-2}). It was further shown that the orientation in rectangular schemes, relative to the road axis, is important: SR 3 m/2 m and SR 2 m/3 m have the same tree density, however, SR 2 m/3 m is preferred. The SR 3 m/2 m scheme has only the acoustic performance of SC 3 m.

Thirdly, pollarded trees are of special interest as they can attain large stem diameters at high densities and they have a limited amount of biomass in the canopy due to the cyclic removal of the branches and foliage. As a result, the possible negative effects of downward scattering will be limited. Another interesting property is that many tree genera suitable for pollarding (e.g. *Salix* and *Populus*) are fast growing. In case high stem diameters can be realized and one has to deal with high-speed road traffic, a FCC scheme should be preferred upon a SC scheme: for a same tree density, a higher insertion loss is obtained.

It is indicated in Fig. 6 whether the combinations of planting schemes, tree spacing, and tree stem diameters are practically achievable. Given the complexity in assessing this, three categories were defined based on the considerations in previous sections. When the surface taken by the stem cross-sections is smaller than 100 m^2/ha (equivalent to 1 percent stem cover), no practical problems are expected (white-filled markers). At the other hand, values above 2 percent are considered to be rather unrealistic (black-filled markers). Between 1 percent and 2 percent, tree belts might be achieved when selecting for species that can be densely planted or develop large stem diameters. Another option is leaving out some rows to obtain an averaged smaller tree base area density (note that the values given here are based on fully populated grids).

The highest total A-weighted road traffic noise insertion loss (on condition that the stem cross-section area stays below 1 percent) is observed when applying a SC 1 m 11 cm scheme. Another practical solution is a SR 2 m/3 m 22 cm scheme: a performance equivalent to a noise barrier with a height of 1 m on grassland is possible, when also allowing for a shrub layer. For a light vehicle at 70 km/h, a traffic noise reduction of near 5 dBA can be achieved (without a shrub layer) with a limited belt depth of only 15 m. Such a scheme can be realized with common species, and has a basal area of only 63 m^2/ha. The FCC 2 m 22 cm has a traffic noise insertion loss which is 0.5 dBA higher, however, the stem base areal

density is very close (95 m^2/ha) to the maximum set value here. Tree stems with diameters of 44 cm are less interesting when combining acoustical efficiency and practical achievability.

7. Conclusions

In this study, the 3D finite-difference time-domain method is used to simulate sound propagation through an infinitely long and 15-m deep vegetation belt along a road. A representative strip of the vegetation belt is considered and mirror planes are placed at the simulation boundaries, normal to the road axis. Preliminary calculations showed that the latter is a sound approach to model an infinitely wide vegetation belt. The computational cost was further reduced by showing that for this specific application and when averaging over a receiver zone, assigning the engine and rolling noise source power to the engine noise source height only (in the Harmonoise/Imagine road traffic noise emission model) was sufficiently accurate. Furthermore, calculations have been performed for coherent line sources. The use of a (partly) incoherent line source generally results in a slightly increased road traffic insertion loss by the vegetation belt.

The presence of a forest floor alone, compared to sound propagation over grassland, was found to be responsible for a reduction in total traffic noise level for a light vehicle driving at 70 km/h near 3 dBA. The noise reducing effects of the forest floor and the optimal tree stem configuration (among the modeled ones), taking into account practical achievability, were predicted to be of similar importance.

With increasing tree stem diameter, traffic noise insertion loss is more pronounced for each planting scheme considered. Furthermore, with increasing distance between the stems, smaller values were found and the importance of the stem diameter decreases. A tree spacing of 3 m and a stem diameter of 11 cm can be considered as the starting point of having positive effects (near 0.5 dBA for a light vehicle at 70 km/h). Note that even for such sparse vegetation, positive ground effects could be expected. The spacing parallel to the road axis was shown to be most important in predicting road traffic noise shielding.

To model the interaction between sound and shrubs, a uniform distribution of scattering cells is assumed. The porosity taken by woody shrub material is estimated based on typical values for the above-ground biomass per unit surface area and allometric relationships. A 2 m-high shrub zone with a length of 15 m, for total above-ground dry biomass of 4 kg/m^2, gives an average road traffic noise insertion loss of 4.7 dBA for a light vehicle at 70 km/h at typical ear heights when referenced to sound propagation over grassland. For an equal amount of biomass per unit surface area, there is a preference for either low shrubs (0.5 m) or higher shrubs (2 m).

Scattering from tree crowns leads to downward scattering of sound, given the low source height and receiver height below the canopy, at close distance. Depending on the parameters used for the specific distribution of scattering elements in the tree crown, the predicted negative effects range from -0.8 to -0.4 dBA for a light vehicle at 70 km/h. With increasing vehicle speed, downward scattering increases. Measurements of road traffic noise scattering near a highway noise barrier including a row of trees (described in another study) fall in the predicted range.

The effect of the presence of tree crowns, shrubs and tree stems was found to be approximately additive. Errors made by adding the insertion losses of the individual layers in the vegetation belt, and thus not explicitly modeling combinations, were smaller than 0.7 dBA for receiver heights ranging from 1 m to 2 m.

Simulations showed that inducing some (pseudo)randomness, either in stem center location, tree diameter, or by omitting a number of rows (assuming that the same forest floor develops in the open zones) hardly affects the insertion loss values. This is interesting from the viewpoint of practical realizations of tree stands, given the inherent randomness in working with living material. Note that in the current mirror-plane approach, only randomness in a direction normal to the road could be considered. Furthermore, omitting some rows in a tree stem grid could allow for local denser zones, still having realistic averaged stem base areal densities. It could be concluded that realistically achievable 15-m deep vegetation belts could compete with the traffic noise insertion loss of a thin, classical noise barrier (on grassland) with a height of 1–1.5 m in a non-refracting atmosphere. The vegetation belt has additional non-acoustic advantages such as being CO$_2$-neutral or positive, having a much higher esthetic value, and its potential to improve local air quality, e.g. by capturing road traffic-originated fine particles.

As a final remark, it has to be stressed that the current study is a purely numerical one. Although a full-wave 3D numerical model has been used, and input parameters in the model are as much as possible based on measured data, validation with measurements at vegetation belts is not provided.

Appendix A. Testing mirror plane approach

The mirror plane approach is checked by means of two dimensional calculations. Insertion loss values for 1/3-octave bands (with central frequencies ranging from 25 Hz to 1600 Hz) using a representative strip only in between two perfectly
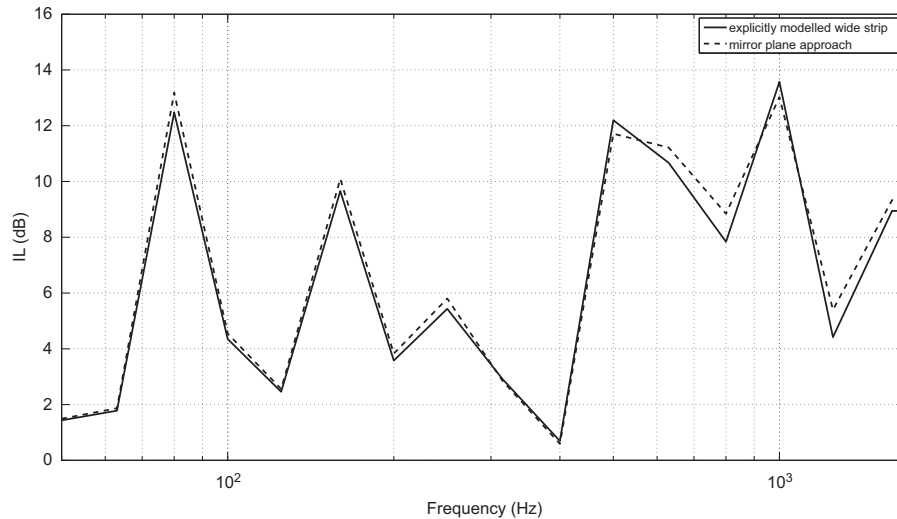
Fig. A.1. Coherent plane wave insertion loss spectrum of a representative strip (using the mirror plane approach) and an explicitly modeled wide SC 1 m/ 2 m 44 cm grid. Absorbing cylinders were considered.

reflecting planes are compared to the results of explicitly modeling a wide strip applying the same scheme. This wide strip is also bordered by reflecting planes at the simulation boundaries along the *x*-axis. In such 2D calculations, coherent plane waves are modeled, parallel to the infinitely long cylinders, in absence of a reflecting ground plane. The number of time steps is kept the same in both situations to have the same amount of reflected energy.

In Fig. A.1, the insertion loss spectrum is shown in the middle of the minimal representative strip of an SR 1 m/2 m 44 cm scheme consisting of partly absorbing cylinders (bark impedance). The corresponding data in case of an explicitly modeled wider strip is shown as well. The results are in good agreement. Only at higher frequencies, small differences are observed. Receiver patterns of insertion losses are also repeated when a wide strip is modeled (not shown).

Appendix B. Calculations with two source heights vs. single source height

The Harmonoise/Imagine (H/I) source power model needs calculations for two source heights. However, since this doubles the number of calculations needed to assess traffic noise insertion loss, it is checked whether the total traffic noise source power (which is the energetic frequency-dependent sum of rolling noise and engine noise) could be assigned completely to the highest source position. For comparison, the H/I model is applied as prescribed, namely sound propagation from both the rolling noise height and engine noise height is explicitly modeled, and the dedicated source power level is assigned to the corresponding source heights, and finally results are energetically summed.

Fig. B.1 shows the average IL in the receiver plane for a type 1 vehicle (light vehicles) as a function of driving speed, calculated with one and two source heights, respectively. When referenced to grassland, taking into account calculations at two source heights, results in slightly higher insertion losses (< 0.5 dBA), especially at the higher vehicle speeds. The single source height approach is therefore considered as sufficiently accurate and is applied in this numerical study, and will result in a slight underprediction of traffic noise insertion losses. Averaging over a range of receiver heights is a possible reason that relaxes the need to explicitly model multiple source heights.

Appendix C. Effect of source type

An incoherent line source is a better representation of a traffic line source. Therefore, the effect of introducing incoherence in the source is compared to a fully coherent line source for some planting schemes. This is modeled in FDTD by assigning a random phase at each point source constituting the line source. In case of a coherent line source, on the other hand, all these pressure points are in phase. In the representative strip approach, however, only incoherence in the representative strip can be modeled. Giving the fact that both the source and planting scheme are mirrored by the reflecting planes at $x=0$ and w_{rs}, a partly incoherent line source is actually modeled. The mirrored part of the line source is again in phase with the explicitly modeled part of the line source. However, this approach allows studying the importance of source type.

Given the random nature involved, each simulation for the partly incoherent line source is performed for 5 realizations and (linearly) averaged afterwards. The influence of source type has been investigated for 3 different planting schemes, each time for a stem diameter of 22 cm and 44 cm. The difference in average insertion loss between a coherent and (partly) incoherent line source, in function of vehicle speed, is shown in Fig. C.1.
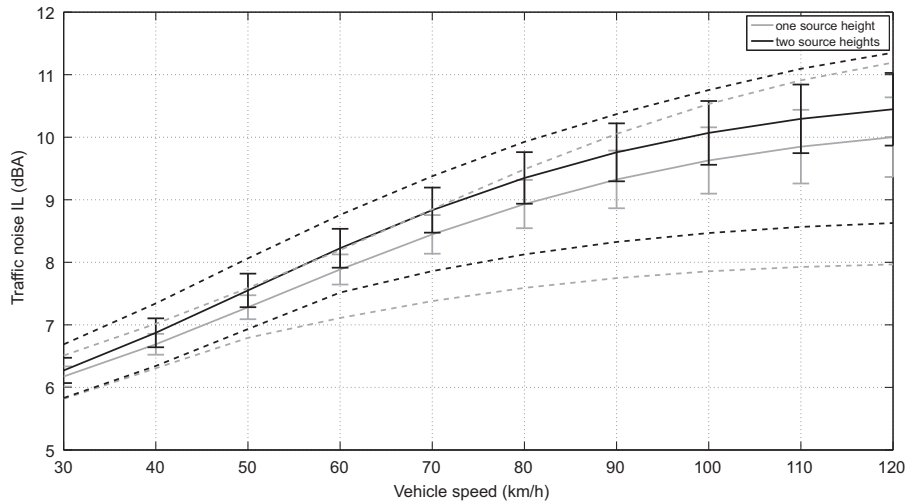
Fig. B.1. Difference in averaged traffic noise IL (referenced to grass-covered soil) for a simulation using a single source height and two source heights as prescribed by the H/I road traffic source power model. The SR 1 m/2 m 44 cm scheme is considered, with receiver heights between 1 m and 2 m. The dashed lines show the minimum and maximum IL found in the receiver plane. The error bars have a total length of two times the standard deviation.
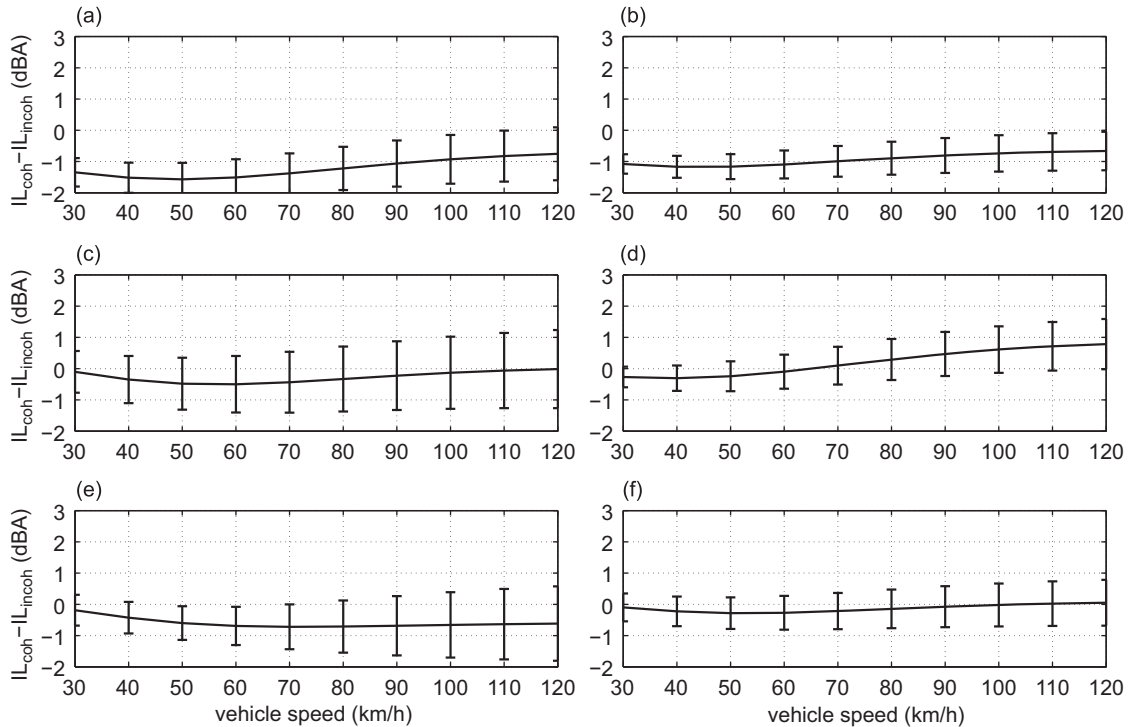
Fig. C.1. Difference in traffic noise IL (light vehicle) between a coherent line source and a (partly) incoherent line source, averaged over the receiver plane (for receivers between 1 m and 2 m), with increasing vehicle speed. The error bars have a total length of two times the standard deviation. The reference situation is here sound propagation over ground as appears under vegetation. Schemes considered: (a) T 2 m 44 cm, (b) T 2 m 22 cm, (c) SR 1 m/2 m 44 cm, (d) SR 1 m/2 m 22 cm, (e) SC 2 m 44 cm and (f) SC 2 m 22 cm.

It can be concluded that an incoherent line source does not result in overall lower insertion loss values when compared to the same type of ground, in contrast to what is observed, e.g. near noise screens [57,58]. In most cases, the incoherent line source representation gives a somewhat higher traffic noise insertion loss. Furthermore, this difference is vehicle-speed dependent. Only for the SR 1 m/2 m 22 cm scheme, a coherent line source gives a slightly higher insertion loss at vehicle speeds exceeding 70 km/h. The averaged differences are mostly limited to within 1 dBA. Modeling a coherent line source as is performed in this paper will typically lead to a slight underprediction of the traffic noise insertion loss.

Table D1

Overview of simulation results for total traffic noise reduction (in dBA) of different tree stems orderings and parameters, for light vehicle speeds of 30 km/h, 70 km/h, and 110 km/h, referenced to sound propagation over the same type of soil (vegetation soil) or grassland, in absence of tree stems. The values in between brackets are the standard deviation on the data in the receiver zones considered. A coherent line source is used. Stem diameters are constant, and shifts of the stem axis from the planting scheme considered are absent unless explicitly indicated. Details on the exact locations of the gaps are found in Fig. 12; the parameter choice as for the randomness in stem center location and diameter can be found in Section 5.8.

Scheme	Spacing	Stem diameter (cm)	Stem height (m)	Number of rows	Additional information	30 km/h			70 km/h			110 km/h		
						Veg. soil (0–3 m)	Veg. soil (1–2 m)	Grass (1–2 m)	Veg. soil (0–3 m)	Veg. soil (1–2 m)	Grass (1–2 m)	Veg. soil (0–3 m)	Veg. soil (1–2 m)	Grass (1–2 m)
FCC	2 m	11	2.5	11		0.2 (0.1)	0.3 (0.1)	3 (0.1)	0.8 (0.3)	1 (0.2)	4.2 (0.4)	1.1 (0.4)	1.4 (0.3)	4.7 (0.7)
FCC	2 m	22	2.5	11		0.5 (0.2)	0.5 (0.1)	3.3 (0.1)	1.5 (0.6)	1.9 (0.3)	5.1 (0.4)	2.2 (0.8)	2.8 (0.5)	6.1 (0.7)
FCC	2 m	44	2.5	11		0.8 (0.6)	0.9 (0.2)	3.6 (0.1)	2.5 (1.1)	2.9 (0.4)	6.1 (0.2)	3.8 (1.3)	4.5 (0.4)	7.8 (0.5)
SC	1 m	11	2.5	16		0.6 (0.1)	0.7 (0.1)	3.4 (0.1)	1.6 (0.6)	2.1 (0.2)	5.3 (0.4)	2.4 (0.8)	3.1 (0.3)	6.4 (0.7)
SC	1 m	22	2.5	16		1.1 (0.5)	1.1 (0.2)	3.8 (0.1)	2.6 (1.1)	2.8 (0.3)	6.1 (0.4)	3.7 (1.3)	4.2 (0.5)	7.5 (0.8)
SC	1 m	44	2.5	16		2.5 (1.8)	2.4 (0.7)	5.1 (0.5)	4.7 (2.7)	4.8 (0.8)	8 (0.6)	6.6 (3)	6.9 (0.7)	10.2 (0.3)
SC	2 m	11	2.5	8		0.2 (0.1)	0.3 (0.1)	3 (0.1)	0.7 (0.5)	0.9 (0.5)	4.1 (0.6)	1 (0.7)	1.3 (0.7)	4.6 (0.9)
SC	2 m	22	2.5	6	Gaps, realization a	0.5 (0.2)	0.5 (0.1)	3.3 (0.1)	1.3 (0.5)	1.6 (0.3)	4.8 (0.4)	1.8 (0.6)	2.2 (0.4)	5.5 (0.7)
SC	2 m	22	2.5	6	Gaps, realization b	0.5 (0.2)	0.5 (0.1)	3.2 (0.1)	1.2 (0.6)	1.5 (0.4)	4.8 (0.5)	1.7 (0.8)	2.1 (0.6)	5.5 (0.9)
SC	2 m	22	2.5	6	Gaps, realization c	0.5 (0.2)	0.5 (0.1)	3.2 (0.1)	1.2 (0.5)	1.5 (0.3)	4.7 (0.5)	1.6 (0.6)	2 (0.4)	5.3 (0.7)
SC	2 m	22	2.5	6	Gaps, realization d	0.5 (0.2)	0.5 (0.1)	3.3 (0.1)	1.3 (0.6)	1.6 (0.4)	4.8 (0.5)	1.8 (0.8)	2.2 (0.7)	5.5 (0.9)
SC	2 m	22	2.5	8	Stem center shifts	0.6 (0.3)	0.6 (0.1)	3.3 (0.1)	1.5 (0.6)	1.9 (0.4)	5.1 (0.4)	2.1 (0.8)	2.6 (0.5)	5.9 (0.8)
SC	2 m	22	2.5	8		0.6 (0.2)	0.6 (0.1)	3.3 (0.1)	1.4 (0.6)	1.8 (0.3)	5 (0.4)	2 (0.7)	2.5 (0.5)	5.8 (0.7)
SC	2 m	44	2.5	6	Gaps, realization a	1.3 (0.3)	1.4 (0.1)	4.1 (0.1)	2.4 (0.8)	2.7 (0.4)	6 (0.5)	3.2 (0.9)	3.6 (0.7)	6.9 (0.9)
SC	2 m	44	2.5	6	Gaps, realization b	1.3 (0.3)	1.4 (0.1)	4.1 (0.1)	2.5 (0.8)	2.8 (0.4)	6 (0.5)	3.3 (0.9)	3.7 (0.7)	7 (0.9)
SC	2 m	44	2.5	6	Gaps, realization c	1.4 (0.4)	1.4 (0.2)	4.1 (0.1)	2.5 (0.9)	2.8 (0.6)	6 (0.7)	3.3 (1.1)	3.7 (1)	7 (1.2)
SC	2 m	44	2.5	6	Gaps, realization d	1.4 (0.3)	1.4 (0.1)	4.1 (0.1)	2.5 (0.8)	2.8 (0.5)	6 (0.5)	3.3 (1)	3.7 (0.8)	7 (0.9)
SC	2 m	44	2.5	8	Stem center shifts	1.4 (0.4)	1.5 (0.2)	4.2 (0.1)	2.6 (0.9)	2.9 (0.6)	6.2 (0.6)	3.5 (1.2)	3.9 (1)	7.2 (1.2)
SC	2 m	44	2.5	8		1.5 (0.4)	1.5 (0.2)	4.3 (0.1)	2.5 (1)	2.7 (0.7)	6 (0.8)	3.2 (1.3)	3.5 (1.2)	6.9 (1.3)
SC	2 m	22–44	2.5	8	Random stem diameter	1 (0.3)	1 (0.1)	3.8 (0.1)	2.1 (0.8)	2.4 (0.5)	5.6 (0.5)	2.8 (1)	3.2 (0.8)	6.6 (1)
SC	3 m	22	2.5	6		0.3 (0.1)	0.3 (0.1)	3 (0.1)	0.7 (0.4)	0.9 (0.4)	4.1 (0.6)	1 (0.6)	1.2 (0.7)	4.6 (0.9)
SC	3 m	44	2.5	6		0.8 (0.2)	0.8 (0.1)	3.5 (0.1)	1.5 (0.9)	1.6 (1)	4.9 (1)	2 (1.4)	2.3 (1.6)	5.6 (1.7)
SC	3 m	11	2.5	6		0.1 (0.1)	0.1 (0.1)	2.9 (0.1)	0.3 (0.2)	0.4 (0.2)	3.7 (0.5)	0.5 (0.3)	0.6 (0.2)	3.9 (0.7)
SR	1 m/2 m	11	2.5	8		0.4 (0.1)	0.5 (0.1)	3.2 (0.1)	1.1 (0.4)	1.4 (0.2)	4.7 (0.4)	1.6 (0.5)	2 (0.3)	5.3 (0.6)
SR	1 m/2 m	22	2.5	2		0.5 (0)	0.5 (0)	1.5 (0)	1.1 (0.2)	1.1 (0.1)	3.1 (0.1)	1.4 (0.2)	1.5 (0.2)	3.9 (0.2)
SR	1 m/2 m	22	2.5	4		0.7 (0.1)	0.6 (0.1)	2.2 (0.1)	1.7 (0.4)	1.7 (0.2)	4.4 (0.2)	2.4 (0.5)	2.5 (0.3)	5.6 (0.4)
SR	1 m/2 m	22	2.5	6	Gaps, realization a	0.9 (0.2)	1 (0.1)	3.7 (0.1)	2.2 (0.8)	2.7 (0.3)	5.9 (0.3)	3.2 (1)	3.9 (0.4)	7.2 (0.6)
SR	1 m/2 m	22	2.5	6	Gaps, realization b	0.8 (0.2)	0.9 (0.1)	3.6 (0.1)	2.1 (0.7)	2.5 (0.3)	5.8 (0.4)	3 (0.9)	3.7 (0.5)	7 (0.7)
SR	1 m/2 m	22	2.5	6	Gaps, realization c	0.8 (0.2)	0.9 (0.1)	3.6 (0.1)	2 (0.7)	2.4 (0.3)	5.7 (0.4)	2.8 (0.9)	3.4 (0.5)	6.8 (0.8)
SR	1 m/2 m	22	2.5	6	Gaps, realization d	0.9 (0.2)	0.9 (0.1)	3.7 (0.1)	2.1 (0.7)	2.6 (0.3)	5.8 (0.4)	3 (0.9)	3.7 (0.4)	7 (0.7)
SR	1 m/2 m	22	2.5	6		0.8 (0.2)	0.8 (0.1)	2.7 (0.1)	2 (0.6)	2.2 (0.3)	5.1 (0.4)	2.8 (0.7)	3.3 (0.4)	6.4 (0.4)
SR	1 m/2 m	22	0.5	8		0.3 (0.2)	0.4 (0.1)	3.1 (0.1)	0.9 (0.3)	1.1 (0.1)	4.4 (0.4)	1.2 (0.4)	1.6 (0.1)	4.9 (0.6)
SR	1 m/2 m	22	1	8		0.6 (0.4)	0.7 (0.1)	3.4 (0)	1.5 (0.8)	2 (0.3)	5.2 (0.3)	2.1 (1)	2.8 (0.3)	6.2 (0.6)
SR	1 m/2 m	22	1.5	8		0.7 (0.4)	0.8 (0.2)	3.5 (0.1)	1.8 (1)	2.2 (0.5)	5.4 (0.2)	2.5 (1.2)	3.2 (0.6)	6.5 (0.4)
SR	1 m/2 m	22	2	8		0.8 (0.4)	0.8 (0.2)	3.6 (0.1)	2 (0.9)	2.3 (0.4)	5.5 (0.4)	2.9 (1.1)	3.3 (0.5)	6.6 (0.7)
SR	1 m/2 m	22	2.5	8	Stem center shifts	1 (0.3)	1 (0.1)	3.8 (0)	2.6 (0.9)	3.1 (0.3)	6.3 (0.3)	3.8 (1.2)	4.6 (0.4)	8 (0.6)
SR	1 m/2 m	22	2.5	8		1 (0.3)	1 (0.1)	3.8 (0.1)	2.3 (0.8)	2.8 (0.3)	6 (0.4)	3.2 (1)	4 (0.5)	7.3 (0.7)
SR	1 m/2 m	44	2.5	2		1.9 (0.1)	1.9 (0.1)	2.9 (0.1)	2.9 (0.3)	3 (0.3)	5 (0.3)	3.6 (0.5)	3.7 (0.5)	6.1 (0.5)
SR	1 m/2 m	44	2.5	4		2.5 (0.2)	2.5 (0.1)	4 (0.1)	3.8 (0.6)	3.9 (0.3)	6.5 (0.2)	4.8 (0.7)	5 (0.5)	8 (0.4)
SR	1 m/2 m	44	2.5	6	Gaps, realization a	3.2 (0.4)	3.2 (0.2)	5.9 (0.1)	4.9 (1.1)	5.3 (0.4)	8.6 (0.2)	6.3 (1.3)	7 (0.4)	10.4 (0.6)

SR	1 m/2 m	44	2.5	6	Gaps, realization b	3.1 (0.5)	3.2 (0.2)	5.9 (0.1)	4.8 (1.1)	5.2 (0.4)	8.4 (0.3)	6.2 (1.3)	6.7 (0.4)	10.1 (0.6)
SR	1 m/2 m	44	2.5	6	Gaps, realization c	3.3 (0.5)	3.3 (0.2)	6 (0.1)	4.7 (1.1)	5 (0.4)	8.2 (0.3)	5.8 (1.2)	6.2 (0.5)	9.6 (0.7)
SR	1 m/2 m	44	2.5	6	Gaps, realization d	3.3 (0.4)	3.3 (0.2)	6 (0.1)	5 (1.1)	5.3 (0.4)	8.6 (0.3)	6.4 (1.3)	7 (0.4)	10.3 (0.6)
SR	1 m/2 m	44	2.5	6		2.9 (0.5)	2.9 (0.2)	4.9 (0.2)	4.3 (1)	4.5 (0.5)	7.4 (0.2)	5.3 (1.3)	5.9 (0.6)	9 (0.4)
SR	1 m/2 m	44	0.5	8		1.1 (0.3)	1.2 (0.1)	3.9 (0)	2 (0.6)	2.5 (0.1)	5.7 (0.4)	2.8 (0.7)	3.4 (0.1)	6.8 (0.7)
SR	1 m/2 m	44	1	8		2.2 (0.7)	2.4 (0.3)	5.1 (0.2)	3.8 (1.3)	4.6 (0.4)	7.8 (0.2)	5 (1.6)	6.4 (0.3)	9.7 (0.5)
SR	1 m/2 m	44	1.5	8		2.8 (0.9)	3 (0.4)	5.7 (0.3)	4.5 (1.7)	5.3 (0.7)	8.5 (0.3)	5.8 (2.1)	7.1 (0.9)	10.4 (0.5)
SR	1 m/2 m	44	2	8		3.2 (0.9)	3.2 (0.4)	5.9 (0.3)	4.8 (1.7)	5.1 (0.7)	8.3 (0.4)	6 (2)	6.5 (0.9)	9.8 (0.5)
SR	1 m/2 m	44	2.5	8	Stem center shifts	3.3 (0.7)	3.3 (0.3)	6.1 (0.2)	5.4 (1.5)	5.7 (0.5)	8.9 (0.1)	7.1 (1.7)	7.8 (0.4)	11.1 (0.3)
SR	1 m/2 m	44	2.5	8		3.5 (0.7)	3.5 (0.3)	6.2 (0.2)	5 (1.4)	5.2 (0.5)	8.4 (0.3)	6.1 (1.6)	6.5 (0.6)	9.8 (0.6)
SR	1 m/2 m	22–44	2.5	8	Random stem diameter	2.1 (0.5)	2.2 (0.2)	4.9 (0.1)	3.9 (1.2)	4.2 (0.4)	7.5 (0.2)	5.1 (1.4)	5.8 (0.4)	9.2 (0.5)
SR	1 m/3 m	11	2.5	6		0.3 (0.1)	0.4 (0.1)	3.1 (0.1)	0.9 (0.4)	1.2 (0.2)	4.4 (0.4)	1.3 (0.5)	1.7 (0.3)	5 (0.7)
SR	1 m/3 m	22	2.5	6		0.8 (0.2)	0.9 (0.1)	3.6 (0.1)	2.1 (0.7)	2.5 (0.3)	5.8 (0.4)	3 (0.9)	3.8 (0.4)	7.1 (0.7)
SR	1 m/3 m	44	2.5	6		2.6 (0.4)	2.6 (0.2)	5.3 (0.1)	4.3 (1)	4.7 (0.4)	8 (0.5)	5.9 (1.3)	6.6 (0.6)	9.9 (0.8)
SR	2 m/1 m	11	2.5	8		0.4 (0.1)	0.5 (0.1)	3.2 (0.1)	1.1 (0.5)	1.5 (0.3)	4.7 (0.5)	1.6 (0.7)	2.1 (0.5)	5.4 (0.8)
SR	2 m/1 m	22	2.5	8		0.7 (0.3)	0.7 (0.1)	3.4 (0.1)	1.6 (0.8)	1.8 (0.5)	5.1 (0.4)	2.2 (1.1)	2.6 (1.1)	5.9 (1.2)
SR	2 m/1 m	44	2.5	8		1.3 (0.8)	1.2 (0.3)	4 (0.2)	2.3 (1.4)	2.5 (0.9)	5.7 (0.9)	3.1 (1.7)	3.5 (1.4)	6.8 (1.5)
SR	2 m/3 m	11	2.5	6		0.2 (0.1)	0.2 (0.1)	2.9 (0.1)	0.5 (0.4)	0.7 (0.4)	3.9 (0.6)	0.8 (0.6)	1 (0.6)	4.3 (0.8)
SR	2 m/3 m	22	2.5	6		0.5 (0.2)	0.5 (0.1)	3.2 (0.1)	1.2 (0.6)	1.5 (0.4)	4.8 (0.5)	1.7 (0.7)	2.1 (0.6)	5.5 (0.9)
SR	2 m/3 m	44	2.5	6		1.2 (0.3)	1.2 (0.1)	3.9 (0.1)	2.4 (0.8)	2.7 (0.5)	5.9 (0.6)	3.2 (1.1)	3.7 (0.9)	7 (1)
SR	3 m/1 m	11	2.5	16		0.3 (0.1)	0.3 (0.1)	3 (0.1)	0.7 (0.5)	0.9 (0.5)	4.2 (0.6)	1 (0.7)	1.3 (0.8)	4.6 (1)
SR	3 m/1 m	22	2.5	16		0.5 (0.3)	0.5 (0.2)	3.2 (0.2)	1.1 (1.1)	1.2 (1.2)	4.4 (1.2)	1.5 (1.7)	1.7 (1.9)	5.1 (2)
SR	3 m/1 m	44	2.5	16		0.9 (0.5)	0.9 (0.3)	3.6 (0.3)	1.6 (1.5)	1.7 (1.5)	4.9 (1.5)	2.2 (2.2)	2.4 (2.4)	5.8 (2.4)
SR	3 m/2 m	11	2.5	8		0.2 (0.1)	0.2 (0.1)	2.9 (0.1)	0.4 (0.3)	0.6 (0.3)	3.8 (0.5)	0.6 (0.4)	0.8 (0.3)	4.1 (0.7)
SR	3 m/2 m	22	2.5	8		0.4 (0.2)	0.4 (0.1)	3.1 (0.1)	0.9 (0.6)	1.1 (0.6)	4.3 (0.7)	1.2 (0.9)	1.5 (1)	4.8 (1.2)
SR	3 m/2 m	44	2.5	8		1 (0.3)	1 (0.2)	3.7 (0.2)	1.6 (1.1)	1.7 (1.2)	4.9 (1.3)	2.1 (1.7)	2.3 (1.9)	5.6 (2)
T	2 m	11	2.5	11		0.2 (0.1)	0.3 (0)	3 (0.1)	0.7 (0.3)	0.9 (0.1)	4.2 (0.4)	1 (0.3)	1.3 (0.2)	4.6 (0.6)
T	2 m	22	2.5	11		0.5 (0.2)	0.6 (0.1)	3.3 (0.1)	1.4 (0.6)	1.7 (0.3)	5 (0.4)	2 (0.7)	2.4 (0.4)	5.7 (0.7)
T	2 m	44	2.5	11		1.2 (0.6)	1.2 (0.2)	3.9 (0.1)	2.8 (1.2)	3.2 (0.5)	6.4 (0.4)	4 (1.4)	4.7 (0.6)	8 (0.7)

Table D2
See caption of Table D.1, but now for different shrub parameters and noise walls (with a thickness of 0.1 m, at 3 m from the line source).

Shrub height (m)	Shrub porosity	Noise screen height (m)	30 km/h			70 km/h			110 km/h		
			Veg. soil (0–3 m)	Veg. soil (1–2 m)	Grass (1–2 m)	Veg. soil (0–3 m)	Veg. soil (1–2 m)	Grass (1–2 m)	Veg. soil (0–3 m)	Veg. soil (1–2 m)	Grass (1–2 m)
0.5	0.98	–	1.6 (0.2)	1.8 (0)	4.5 (0.1)	2.1 (0.5)	2.5 (0)	5.7 (0.5)	2.4 (0.8)	3.1 (0.1)	6.4 (0.7)
1	0.99	–	1.3 (0.2)	1.4 (0.1)	4.1 (0.1)	1 (0.9)	1.4 (0.4)	4.7 (0.2)	0.9 (1.5)	1.6 (0.6)	4.9 (0.2)
1.5	0.9933	–	1.2 (0.1)	1.1 (0.1)	3.8 (0.1)	1.1 (0.3)	0.8 (0.2)	4 (0.4)	1.2 (0.5)	0.6 (0.3)	3.9 (0.5)
2	0.995	–	1.2 (0.1)	1.2 (0.1)	4 (0.2)	1.3 (0.3)	1.5 (0.4)	4.7 (0.8)	1.5 (0.4)	1.7 (0.5)	5 (1.2)
0.5	0.99	–	0.8 (0.1)	0.9 (0)	3.6 (0.1)	0.9 (0.4)	1.1 (0.1)	4.3 (0.4)	0.9 (0.7)	1.3 (0.1)	4.6 (0.5)
1.5	0.99	–	1.8 (0.1)	1.7 (0.1)	4.4 (0)	1.7 (0.4)	1.2 (0.4)	4.4 (0.2)	1.7 (0.7)	1 (0.6)	4.3 (0.3)
2	0.99	–	2.3 (0.2)	2.4 (0.2)	5.1 (0.3)	2.5 (0.5)	2.7 (0.7)	5.9 (1.2)	2.8 (0.8)	3 (1.1)	6.4 (1.7)
0.5	0.995	–	0.4 (0.1)	0.4 (0)	3.1 (0.1)	0.4 (0.2)	0.4 (0.1)	3.7 (0.4)	0.3 (0.4)	0.5 (0.1)	3.8 (0.5)
1	0.995	–	0.6 (0.1)	0.6 (0.1)	3.3 (0.1)	0.4 (0.5)	0.5 (0.3)	3.7 (0.2)	0.3 (0.7)	0.4 (0.4)	3.8 (0.3)
1.5	0.995	–	0.9 (0)	0.8 (0)	3.5 (0.1)	0.9 (0.2)	0.6 (0.1)	3.8 (0.4)	0.9 (0.4)	0.5 (0.2)	3.8 (0.6)
–	–	0.5	–	–	1.1 (0.1)	–	–	3.6 (0.1)	–	–	5.2 (0.1)
–	–	1	–	–	3.3 (0.1)	–	–	6.2 (0.1)	–	–	8.3 (0)
–	–	1.5	–	–	5.9 (0.2)	–	–	8.8 (0.2)	–	–	10.7 (0.2)
–	–	2	–	–	7.6 (0.3)	–	–	10.6 (0.4)	–	–	12.8 (0.5)
–	–	2.5	–	–	8.6 (0.3)	–	–	11.7 (0.5)	–	–	14.2 (0.7)

When analyzing band gap behavior in case of an incoherent line source (not shown), the magnitude of the (low-frequency) peaks corresponding to the basic grid spacing are hardly affected. Source incoherence does not destroy the presence of band gap effects in the current setting.

Appendix D. Overview of simulation results

The simulation results appearing in this paper are summarized in Tables D1 and D2.

References

[1] D. Aylor, Noise reduction by vegetation and ground, *Journal of the Acoustical Society of America* 51 (1972) 197–205.
[2] D. Aylor, Sound transmission through vegetation in relation to leaf area density, leaf width, and breadth of canopy, *Journal of the Acoustical Society of America* 51 (1972) 411–414.
[3] J. Kragh, Pilot-study on railway noise attenuation by belts of trees, *Journal of Sound and Vibration* 66 (1979) 407–415.
[4] J. Kragh, Road traffic noise attenuation by belts of trees, *Journal of Sound and Vibration* 74 (1981) 235–241.
[5] R. Bullen, F. Fricke, Sound-propagation through vegetation, *Journal of Sound and Vibration* 80 (1982) 11–23.
[6] A. Pal, V. Kumar, N. Saxena, Noise attenuation by green belts, *Journal of Sound and Vibration* 234 (2000) 149–165.
[7] C. Fang, D. Ling, Investigation of the noise reduction provided by tree belts, *Landscape and Urban Planning* 63 (2003) 187–195.
[8] C. Fang, D. Ling, Guidance for noise reduction provided by tree belts, *Landscape and Urban Planning* 71 (2005) 29–34.
[9] V. Tyagi, K. Kumar, V. Jain, A study of the spectral characteristics of traffic noise attenuation by vegetation belts in Delhi, *Applied Acoustics* 67 (2006) 926–935.
[10] V. Pathak, B. Tripathi, V. Mishra, Dynamics of traffic noise in a tropical city Varanasi and its abatement through vegetation, *Environmental Monitoring and Assessment* 146 (2008) 67–75.
[11] R. Lyon, Evaluating effects of vegetation on the acoustical environment by physical scale-modeling, *Proceedings of the Conference on Metropolitan Physical Environment*, USDA Forest Service General Technical Report NE-2, 1977.
[12] T. Embleton, Sound propagation in homogeneous deciduous and evergreen woods, *Journal of the Acoustical Society of America* 35 (1963) 1119–1125.
[13] M. Martens, A. Michelsen, Absorption of acoustic energy by plant-leaves, *Journal of the Acoustical Society of America* 69 (1981) 303–306.
[14] S. Tang, P. Ong, H. Woon, Monte-Carlo simulation of sound-propagation through leafy foliage using experimentally obtained leaf resonance parameters, *Journal of the Acoustical Society of America* 80 (1986) 1740–1744.
[15] W. Huisman, K. Attenborough, Reverberation and attenuation in a pine forest, *Journal of the Acoustical Society of America* 90 (1991) 2664–2677.
[16] J. Defrance, Forest as a meteorological screen for traffic noise, *Proceedings of the 9th International Congress on Sound and Vibration (ICSV9)*, Orlando, USA, 2002.
[17] A. Tunick, Calculating the micrometeorological influences on the speed of sound through the atmosphere in forests, *Journal of the Acoustical Society of America* 114 (2003) 1796–1806.
[18] M. Swearingen, M. White, Influence of scattering, atmospheric refraction, and ground effect on sound propagation through a pine forest, *Journal of the Acoustical Society of America* 122 (2007) 113–119.
[19] T. Van Renterghem, D. Botteldooren, Effect of a row of trees behind noise barriers in wind, *Acta Acustica United with Acustica* 88 (2002) 869–878.
[20] T. Van Renterghem, D. Botteldooren, Numerical simulation of the effect of trees on downwind noise barrier performance, *Acta Acustica United with Acustica* 89 (2003) 764–778.
[21] T. Van Renterghem, D. Botteldooren, Numerical evaluation of tree canopy shape near noise barriers to improve downwind shielding, *Journal of the Acoustical Society of America* 123 (2008) 648–657.
[22] F. Fricke, Sound-attenuation in forests, *Journal of Sound and Vibration* 92 (1984) 149–158.
[23] O. Fegeant, Wind-induced vegetation noise. Part II: field measurements, *Acta Acustica United with Acustica* 85 (1999) 241–249.
[24] K. Bolin, Prediction method for wind-induced vegetation noise, *Acta Acustica United with Acustica* 95 (2009) 607–619.
[25] S. Viollon, C. Lavandier, C. Drake, Influence of visual setting on sound ratings in an urban environment, *Applied Acoustics* 63 (2002) 493–511.
[26] J. Sanchez-Perez, C. Rubio, R. Martinez-Sala, R. Sanchez-Grandia, V. Gomez, Acoustic barriers based on periodic arrays of scatterers, *Applied Physics Letters* 81 (2002) 5240–5242.

[27] Y.-Y. Chen, Z. Ye, Acoustic attenuation by two-dimensional arrays of rigid cylinders, *Physical Review Letters* 87 (2001) 184301/1–4.
[28] O. Umnova, K. Attenborough, C. Linton, Effects of porous covering on sound attenuation by periodic arrays of cylinders, *Journal of the Acoustical Society of America* 119 (2006) 278–284.
[29] R. Martinez-Sala, C. Rubio, L. Garcia-Raffi, J. Sanchez-Perez, E. Sanchez-Perez, J. Llinares, Control of noise by trees arranged like sonic crystals, *Journal of Sound and Vibration* 291 (2006) 100–106.
[30] D. Heimann, Numerical simulations of wind and sound propagation through an idealised stand of trees, *Acta Acustica United with Acustica* 89 (2003) 779–788.
[31] M. Price, K. Attenborough, N. Heap, Sound-attenuation through trees—measurements and models, *Journal of the Acoustical Society of America* 84 (1988) 1836–1844.
[32] D. Heimann, Three-dimensional linearised Euler model simulations of sound propagation in idealised urban situations with wind effects, *Applied Acoustics* 68 (2007) 217–237.
[33] M. Hornikx, R. Waxler, J. Forssen, The extended Fourier pseudospectral time-domain method for atmospheric sound propagation, *Journal of the Acoustical Society of America* 128 (2010) 1632–1646.
[34] L. Garcia-Raffi, V. Romero-García, J. Sánchez-Pérez, S. Castiñeira-Ibáñez, J. Herrero, S. García-Nieto, X. Blasco, Generation of defects for improving properties of periodic systems, *Proceedings of the 8th European Conference on Noise Control (Euronoise)*, Edinburgh, UK, 2009.
[35] R. Bullen, F. Fricke, Sound propagation through vegetation, *Journal of Sound and Vibration* 80 (1982) 11–23.
[36] A. Krynkin, O. Umnova, The effect of ground on performance of sonic crystal noise barriers, *Proceedings of the 8th European Conference on Noise Control (Euronoise)*, Edinburgh, UK, 2009.
[37] M. Martens, Foliage as a low-pass filter—experiments with model forests in an anechoic chamber, *Journal of the Acoustical Society of America* 67 (1980) 66–72.
[38] C. Zwikker, C. Kosten, *Sound Absorbing Materials*, Elsevier, New York, 1949.
[39] D. Botteldooren, Finite-difference time-domain simulation of low-frequency room acoustic problems, *Journal of the Acoustical Society of America* 98 (1995) 3302–3308.
[40] E. Salomons, R. Blumrich, D. Heimann, Eulerian time-domain model for sound propagation over a finite-impedance ground surface. Comparison with frequency-domain models, *Acta Acustica united with Acustica* 88 (2002) 483–492.
[41] K. Attenborough, I. Bashir, S. Taherzadeh, Outdoor ground impedance models, *Journal of the Acoustical Society of America* 129 (2011) 2806–2819.
[42] G. Reethof, L. Frank, O. McDaniel, Sound absorption characteristics of tree bark and forest floor, *Proceedings of the Conference on Metropolitan Physical Environment*, USDA Forest Service General Technical Report NE-2, 1977.
[43] R. Blumrich, D. Heimann, A linearized Eulerian sound propagation model for studies of complex meteorological effects, *Journal of the Acoustical Society of America* 112 (2002) 446–455.
[44] T. Xiao, Q. Liu, Finite difference computation of head-related transfer functions for human hearing, *Journal of the Acoustical Society of America* 113 (2003) 2434–2441.
[45] L. Liu, D. Albert, Acoustic pulse propagation near a right-angle wall, *Journal of the Acoustical Society of America* 119 (2006) 2073–2083.
[46] H. Jonasson, Acoustical source modelling of road vehicles, *Acta Acustica united with Acustica* 93 (2007) 173–184.
[47] K. Wilson, V. Ostashev, S. Collier, N. Symons, D. Aldridge, D. Marlin, Time-domain calculations of sound interactions with outdoor ground surfaces, *Applied Acoustics* 68 (2007) 173–200.
[48] J. De Poorter, D. Botteldooren, Acoustical finite-difference time-domain simulations of subwavelength geometries, *Journal of the Acoustical Society of America* 104 (1998) 1171–1177.
[49] M. Hornikx, D. Botteldooren, T. Van Renterghem, J. Forssen, Modelling of scattering of sound from trees by the PSTD method, *Proceedings of Forum Acusticum* 2011, Aalborg, Denmark.
[50] R. Navarro-Cerrillo, P. Blanco-Oyonarte, Estimation of above-ground biomass in shrubland ecosystems of southern Spain, *Investigación Agraria: Sistemas y Recursos Forestales* 15 (2006) 197–207.
[51] G. Harrington, Estimation of above-ground biomass of trees and shrubs in a *Eucalyptus populnea* F. Muell. Woodland by regression of mass on trunk diameter and plant height, *Australian Journal of Botany* 27 (1979) 135–143.
[52] J. Navar, E. Mendez, A. Najera, J. Graciano, V. Dale, B. Parresol, Biomass equations for shrub species of Tamaulipan thornscrub of North-eastern Mexico, *Journal of Arid Environments* 59 (2004) 657–674.
[53] M. Sternberg, M. Shoshany, Above-ground biomass allocation and water content relationships in Mediterranean trees and shrubs in two climatological regions in Israel, *Plant Ecology* 157 (2001) 171–179.
[54] L. Butler, J. Cropper, R. Johnson, A. Norman, G. Peacock, P. Shaver, K. Spaeth, *National Range and Pasture Handbook*, United States Department of Agriculture, National Resources Conservation Service, 2003.
[55] H. Martínez-Cabrera, C. Jones, S. Espino, H. Schenk, Wood anatomy and wood density in shrubs: responses to varying aridity along transcontinental transects, *American Journal of Botany* 96 (2009) 1388–1398.
[56] T. Embleton, J. Piercy, N. Olson, Outdoor sound propagation over ground of finite impedance, *Journal of the Acoustical Society of America* 59 (1976) 267–277.
[57] D. Duhamel, Efficient calculation of the three-dimensional sound pressure field around a noise barrier, *Journal of Sound and Vibration* 197 (1996) 547–571.
[58] P. Jean, J. Defrance, Y. Gabillet, The importance of source type on the assessment of noise barriers, *Journal of Sound and Vibration* 226 (1999) 201–216.
[59] E. Salomons, Reduction of the performance of a noise screen due to screen-induced wind-speed gradients. Numerical computations and wind tunnel experiments, *Journal of the Acoustical Society of America* 105 (1999) 2287–2293.
[60] T. Van Renterghem, D. Botteldooren, W. Cornelis, D. Gabriels, Reducing screen-induced refraction of noise barriers in wind with vegetative screens, *Acta Acustica united with Acustica* 88 (2002) 231–238.
[61] L. Reineke, Perfecting a stand-density index for even-aged forest, *Journal of Agricultural Research* 46 (1933) 627–638.